Changes in splicing and neuromodulatory gene expression programs in sensory neurons with pheromone signaling and social experience

Deanhardt Bryson[1*], Duan Qichen[2*], Du Chengcheng[2], Soeder Charles[3], Jones Corbin[3], Volkan Pelin C.[1,2†]

[1]Duke University, Department of Neurobiology

[2]Duke University, Department of Biology

[3]University of Chapel Hill, Department of Biology

*These authors contributed equally

[†]Corresponding Author

Abstract

Social experience and pheromone signaling in ORNs affect pheromone responses and male courtship behaviors in *Drosophila*, however, the molecular mechanisms underlying this circuit-level neuromodulation remain less clear. Previous studies identified social experience and pheromone signaling-dependent modulation of chromatin around behavioral switch gene *fruitless*, which encodes a transcription factor necessary and sufficient for male behaviors. To identify the molecular mechanisms driving social experience-dependent neuromodulation, we performed RNA-seq from antennal samples of mutant fruit flies in pheromone receptors and *fruitless,* as well as grouped or isolated wild-type males. We found that loss of pheromone

detection differentially alters the levels of *fruitless* exons suggesting changes in splicing patterns. In addition, many Fruitless target neuromodulatory genes, such as neurotransmitter receptors, ion channels, and ion transporters, are differentially regulated by social context and pheromone signaling. Our results suggest that modulation of circuit activity and behaviors in response to social experience and pheromone signaling arise due to changes in transcriptional programs for neuromodulators downstream of behavioral switch gene function.

Introduction

Detection of the social environment through pheromone signaling is critical for animals to recalibrate sex-specific behaviors such as mating and aggression (Curley et al., 2011; Cushing and Kramer, 2005; Dey et al., 2015; Sethi et al., 2019). It is thought that changes in social environment can modify the regulation of genes necessary for neuronal homeostasis, physiology, and transmission, ultimately affecting circuit function and behaviors (Cushing and Kramer, 2005; Flavell and Greenberg, 2008; West and Greenberg, 2011). Previous studies on the effects of early life experience have identified changes in neuroanatomy, synaptic plasticity, neurotransmission, and gene expression. For example, maternal licking and grooming of pups, increases DNA methylation around glucocorticoid receptor gene, leading to long-lasting effects on offspring stress responses and behaviors (McGowan et al., 2009; Mifsud et al., 2011; Weaver et al., 2004). However, transcriptional cascades driving in sensory and social experience-dependent modulation of gene expression, circuit function, and behaviors remain unclear.

Identifying gene regulation cascades by which social signals influence neural and behavioral responses requires a model system with well-defined circuits and genetic regulators with roles

44 in neurophysiology, circuit structure, and behavioral function. Courtship circuit and behavior in
45 *Drosophila melanogaster* is an excellent and unique model that provides an experimental
46 system to address this question. In *Drosophila*, male-specific courtship behaviors are governed
47 by a master transcriptional regulator Fruitless^{M} (Fru^{M}), which is encoded by male-specific
48 alternative splicing of the *fruitless* (*fru*) gene from the P1 promoter (Dickson, 2008; Yamamoto
49 and Koganezawa, 2013). It is known that Fru^{M} is both necessary and sufficient for male
50 courtship as loss of Fru^{M} in males leads to a loss of male-female-specific courtship interaction
51 (Demir and Dickson, 2005; Ryner et al., 1996; Von Philipsborn et al., 2014). Fru^{M} is expressed
52 in approximately 2000 interconnected neurons throughout the peripheral and central nervous
53 system and its expression is required for the development, function, and plasticity of the circuit
54 which drives male-specific behaviors (Yamamoto and Kohatsu, 2017). In particular, social cues
55 such as pheromones can affect courtship behaviors in males (Dweck et al., 2015; Kurtovic et
56 al., 2007; Lin et al., 2016; van der Goes van Naters and Carlson, 2007; Yamamoto et al., 2013;
57 Yan et al., 2020). Two types of these pheromones, male-specific pheromone *cis*-vaccenyl
58 acetate and non-sex-specific pheromones (such as methyl laurate and palmitoleic acid),
59 activate Fru^{M}-positive olfactory receptor neurons (ORNs) expressing Or67d and Or47b
60 receptors, respectively (Dweck et al., 2015; Kurtovic et al., 2007; Lin et al., 2016). These two
61 ORN classes act differently, with Or67d regulating male-male repulsive behaviors and
62 aggression, whereas Or47b functioning to drive male-courtship advantage with age and social
63 experience (Dweck et al., 2015; Lin et al., 2016; Sethi et al., 2019; Wang et al., 2011).

64 Previous studies have reported that different social contexts, as well as loss of Or47b or Or67d
65 function, alter the regulation of *fru* transcription, particularly the enrichment of active chromatin
66 marks around *fru* promoters (Hueston et al., 2016; Zhao et al., 2020). In addition, the expression
67 of *fru^{M}* isoforms in Or47b and Or67d ORNs affects physiological responses to pheromone
68 ligands and courtship behaviors (Lin et al., 2016; Ng et al., 2019; Sethi et al., 2019; Zhang and

69 Su, 2020). It is likely that changes in social context, pheromone signaling, as well as
70 subsequent changes in *fru* regulation, affect the expression of ion channels as well as
71 neurotransmitter receptors with functions regulating neurophysiology. Indeed, Fru^M binding is
72 detected upstream of many ion channels and genes controlling neural development and
73 function in the central brain (Nojima et al., 2014; Vernes, 2014). Even though these studies
74 point to the regulation of neuronal and circuit function by Fru^M, very little is known about how it
75 affects the expression of these target genes, or how pheromone signaling and social experience
76 affect transcriptional programs by modulating Fru^M.

77 Here we performed antennal RNA-seq to determine transcriptional changes in response to
78 social isolation and disrupted pheromone receptor signaling or Fru^M function. Our results show
79 that *fru* splicing patterns are also modified in pheromone receptor mutants. We also found that
80 transcriptional programs associated with neuromodulation are altered. Many of the Fru^M target
81 neuromodulatory genes are misregulated in the same direction in fru^M and pheromone receptor
82 mutants. These results are uncover a gene regulatory cascade from pheromone receptors to *fru*
83 regulation, which alter neuromodulatory transcriptional programs to ultimately modulate
84 neuronal and circuit responses in different social contexts.

85

86 Neuronal transcriptional programs are modulated with social 87 isolation and lack of pheromone receptors or Fru^M function.

88 To identify genes regulated in the peripheral olfactory system by social experience, pheromone
89 signaling, and Fru^M, we utilized RNA-seq from whole antennae of 7-day old wild-type (w^{1118})
90 males that are either group-housed (w^{1118} *GH*) or single-housed (w^{1118} *SH*), as well as group-
91 housed *Or47b* mutant males ($Or47b^1$), *Or67d* mutant males ($Or67d^{GAL4}$), and fru^M mutant males

92 (fru^{LexA}/fru^{4-40}) (Figure 1A). Each condition included 3 biological replicates except for fru^{LexA}/fru^{4-40}
93 with only two (Figure 1B). Each sample had mapped reads ranging between 24 and 40 million
94 and hierarchical clustering analysis based on Pearson's correlation between samples shows
95 consistency among replicates within the same genotype (Figure 1B). Principal component
96 analysis (PCA) also shows the expected grouping of the replicates belonging to the same
97 condition, across the first two principal components (PC) accounting for most of the overall
98 variance (32% and 19%) (Figure 1C). We also found that gene expression changes were more
99 similar among *Or67d, Or47b,* and fru^{M} mutants, compared to grouped or isolated wild-type male
100 antennae (Figure 1B,C). As expected, expression levels of *Or47b, Or67d*, and male-specific *fru*
101 exon are significantly lower in all replicates for *Or47b*, Or67d, and fru^{M} mutants, respectively,
102 though the changes of the whole *fru* gene locus cannot be detected (Figure 1D; Figure 4B),
103 validating genotype-specific changes in each condition. In addition, genes known to be absent
104 in adult antennae, such as *amos* (Goulding et al., 2000; Li et al., 2016; zur Lage et al., 2003),
105 also show nearly no expression, whereas housekeeping genes, like *Act5C*, *Gapdh2*, *RpII18*,
106 *fl(2)d*, and *wkd*, show nearly identical expression across all samples (Figure 1D). These results
107 point to high RNA-seq data quality across sample groups and within biological replicates.

108

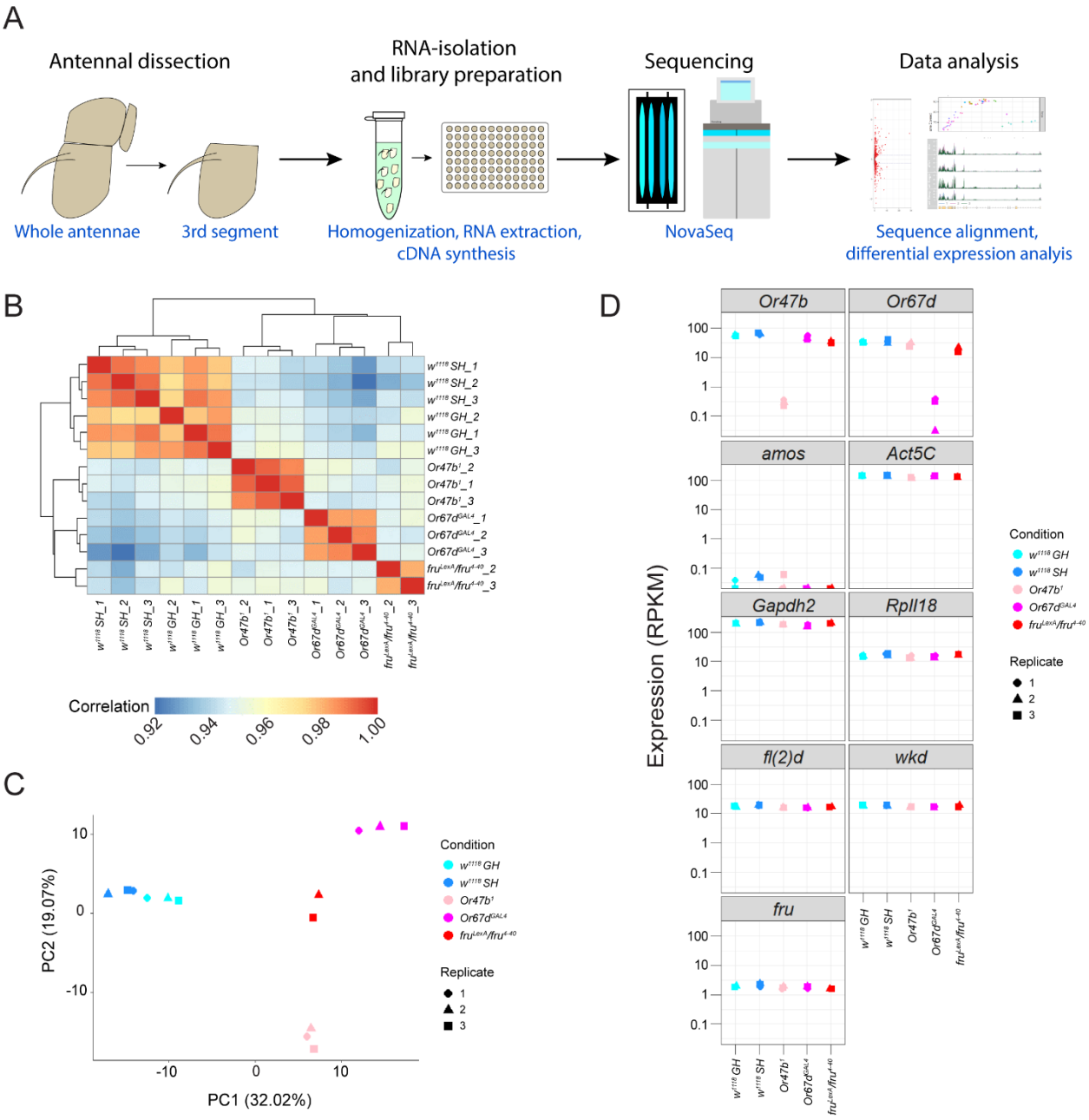

Figure 1. Overview of RNA-seq samples from male antennae. (A) schematic for antennal RNA-seq workflow. **(B-C)** Hierarchical clustering based on Pearson's correlation matrix **(B)** and PCA analysis **(C)** of transcriptional profiles among biological replicates from antennae of wild-type group-housed (*w*^{1118} *GH*), single housed (*w*^{1118} *SH*), and group-housed *Or47b*^{1}, *Or67d*^{GAL4}, and *fru*^{LexA}/*fru*$^{4-40}$ mutant male flies. **(D)** Transcript levels for several representative negative and positive control genes among all samples.

116 We then ran the differential expression analysis to globally examine the transcriptional changes
117 upon loss of social expression, pheromone sensing, or Fru^M function. Compared to group-
118 housed wild-type antennae, social isolation has the least number of significantly altered genes,
119 whereas group-housed *fru^M* mutants resulted in the highest number of significantly differential
120 gene expression (Figure 2A-C). Pairwise comparisons of social deprivation and lack of
121 pheromone receptors/Fru^M function demonstrate the social experience/Or47b/Or67d/Fru^M-
122 dependent transcriptional programs, and notably reveal that the genes co-regulated by
123 pheromone receptors and Fru^M tend to behave in the same direction in the corresponding
124 mutants (Figure 2A,D), suggesting the shared downstream signaling pathways upon pheromone
125 receptor activation and Fru^M-dependent regulation. The numbers of genes with significant
126 differential expression in the same direction shared by each condition compared to the group-
127 housed wild types are illustrated in a Venn diagram and Upset plot (Figure 2B,C), where genes
128 with overlapping changes in social isolation and *Or47b*, *Or67d*, and *fru^M* mutants are
129 highlighted. Particularly, only one gene, *CG13659*, an ecdysteroid kinase-like domain encoding
130 gene, is consistently changed across all experimental conditions compared to antennae from
131 the group-housed wild-type males (Figure 2B).

132 Hierarchical cluster analysis of $\log_2$ fold change versus group-housed wild-type samples shows
133 changes in *fru^M* and *Or67d* mutants as being the most comparable, with single-housed wild
134 types being an outlier of the four groups (Figure 2E). We found that no cluster has a specific
135 bias towards low, medium, or high expression of genes (Figure 2E). Cluster analysis identified
136 several genes of behavioral, neuromodulatory, and developmental importance such as
137 *Cytochrome p450 6a20* (*Cyp6a20*)*, serotonin receptor 2A* (*5-HT2A*)*, Juvenile hormone esterase*
138 (*Jhe*)*,* and *Dpr-interacting protein alpha* (*DIP-alpha*) (Figure 2E) (Carrillo et al., 2015; Johnson et
139 al., 2009; Liu et al., 2008; Wang et al., 2008)*.* Among these, antennal expression of *Cyp6a20,*
140 which is downregulated in *Or47b*, *Or67d*, and *fru^M* mutants, was previously shown to mediate

141 effects of social experience on male-male aggression (Figure 2E) (Wang et al., 2008). On the
142 other hand, *Cyp4p2,* which is involved in hormone metabolism and insecticide detoxification
143 (Scanlan et al., 2020; Seong et al., 2019, 2018), is only misregulated in *Or47b* mutants (Figure
144 2E). In addition to the downregulated genes, we also found some genes encoding ion channels
145 and neurotransmitter receptors that show significant upregulation (*ppk25* and *GluRIIa*) (Figure
146 2E). The heatmap for gene expression changes revealed gene clusters that are co-regulated by
147 pheromone receptors and Fru^M, in addition to gene clusters that are uniquely regulated by each
148 OR and Fru^M; this again highlights that the co-regulated genes tend to change in the same
149 direction in pheromone receptor and *fru* mutants.

150

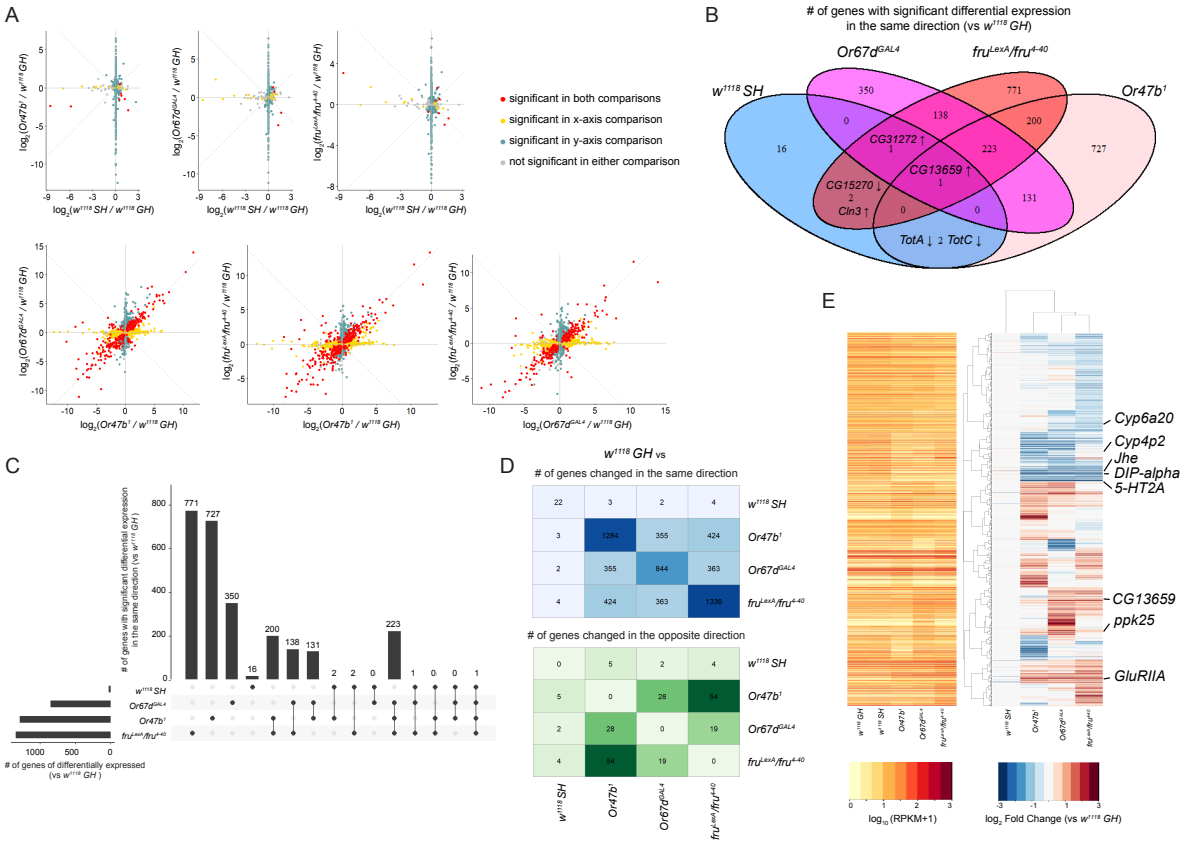

Figure 2. Differentially expressed genes in response to loss of social experience, pheromone receptors, or *fru*^{M}. (A) Scatter plot showing the genes that are differentially regulated among social isolation, and mutants in pheromone receptors and *fru*^{M}. Significance is defined by adjusted p-value below 0.01 after applying Bonferroni correction with n = 2. **(B-C)** Venn diagram **(B)** and UpSet plot **(C)** comparing differentially expressed genes shared across experimental conditions (only genes changed in the same direction). **(D)** Numbers of differentially expressed genes with the same (top) and the opposite (bottom) direction in pairwise comparison of experimental conditions versus group-housed wild-type samples. In (B-D), significance is defined by adjusted p-value below 0.01 after applying Bonferroni correction with n = 4. **(E)** Hierarchically clustered heatmaps showing $\log_2$ fold change compared to group-housed wild-type antennae across all experimental conditions (right) and average mRNA levels (RPKM) of replicates within each condition ordered in the same way as $\log_2$ fold change (left).

164 Only 2999 genes with at least one significant (adjusted p-value below 0.01) change between an

165 experimental condition versus group-housed wild types are shown.

166

167 **Gene ontology terms for differentially expressed genes in**
168 **response to lack of social and pheromone signaling highlight**
169 **neuromodulators**

170 Previous work has demonstrated that social experience, pheromone signaling, and Fru^M activity
171 can regulate the responsiveness of pheromone sensing ORNs to modify circuit function and
172 behavior (Dweck et al., 2015; Kurtovic et al., 2007; Lin et al., 2016; Liu et al., 2011; Sethi et al.,
173 2019; Wang et al., 2008). To functionally understand system-level changes in gene expression
174 with social isolation, lack of pheromone signaling, and *fru*^{M} mutants, we next investigated gene
175 ontology (GO) terms using GOrilla for the list of differentially expressed genes in each
176 experimental condition in pairwise comparisons with group-housed wild types (Eden et al.,
177 2009, 2007) (Figure 3). Many GO terms of molecular function and biological process are
178 commonly affected across multiple experimental groups, suggesting the converging
179 downstream molecular events in response to social experience and pheromone sensing
180 mediated by Fru^M activity (Figure 3). Strikingly, the genes with the altered expression tend to be
181 localized on the cell membrane (Figure 3, GO: cellular component) and have functions in ion
182 transport across membrane (Figure 3, GO: molecular function), and appear to be involved in the
183 process of detecting and responding to olfactory stimuli (Figure 3, GO: biological process). This
184 supports previous studies in providing a general mechanism for social experience, pheromone
185 receptor signaling, and Fru^M-dependent regulation of pheromone responsiveness of Or47b
186 ORNs (Sethi et al., 2019; Zhang et al., 2020; Zhao et al., 2020). Furthermore, genes with
187 oxidoreductase activity also have overlapping alterations across *Or47b*, *Or67d,* and *fru*^{M}
188 mutants, and many of these appear to contribute to insect hormone metabolism (Figure 3, GO:
189 molecular function). Interestingly, previously studies reported that juvenile hormone signaling
190 works together with social experience in olfactory receptor neurons to modulate chromatin

around *fru* locus [4,20]. Our RNA-seq results also add an additional layer of complexity to hormone-social experience interactions, as social experience and pheromone signaling affects the levels of certain hormones by modifying hormone metabolism dynamics. In summary, social isolation, disrupted pheromone receptor signaling, and lack of Fru^M function in peripheral olfactory sensory neurons affect the expression of many genes with roles in diverse aspects of neurophysiology, including neuronal responsiveness, ion transmembrane transport, and beyond.

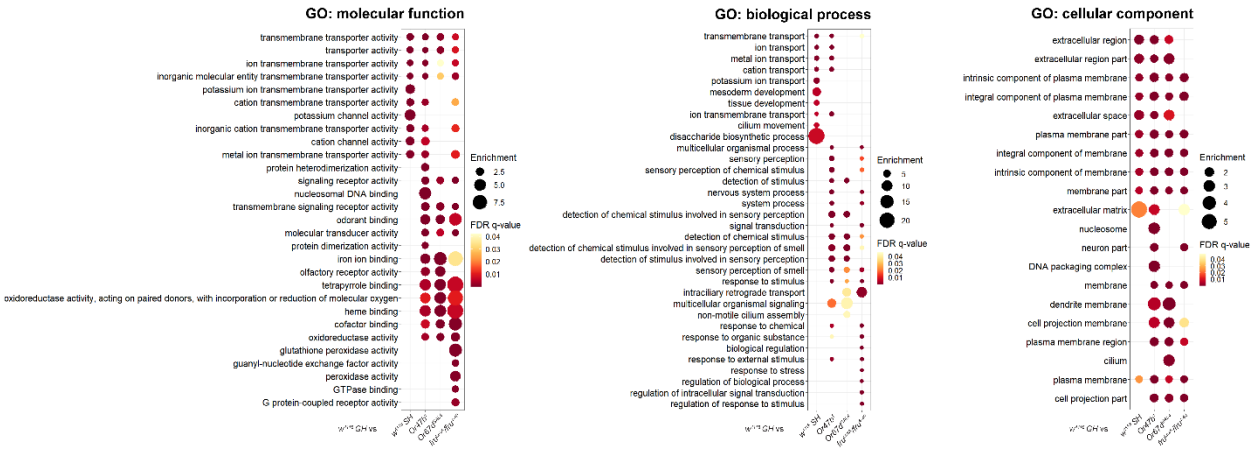

Figure 3. Top enriched gene ontology (GO) terms for differentially expressed genes in response to social experience, pheromone signaling, and Fru^{M} activity. The union set of top 10 most significantly enriched GO terms with FDR q-value below 0.05 of the differentially expressed genes in each experimental condition is shown. Enriched GO terms were generated by the single ranked gene list with the smallest adjusted p-value at the top via GOrilla.

Loss of pheromone signaling alters *fruitless* splicing patterns

Fruitless locus generates multiple alternative splice isoforms for RNAs transcribed from 7 promoters (P1-P6, PD). The transcripts from *fru P1* are alternatively spliced between males and females, where the male, but not the female, isoform (fru^M) encodes functional proteins (Dickson, 2008; Yamamoto and Koganezawa, 2013). The expression of fru^M in males and the absence of functional fru^F transcripts in females help define male and female-specific neuronal pathways as well as the cell-specific expression patterns of genes regulated by Fru^M. Promoter *fru P2* through *fru P6* produce common isoforms in both males and females that also affect sex-specific activity in courtship circuits of both sexes (Goodwin et al., 2000) (Figure 4A). In addition, special transcripts from *fru PD* and *fru P4* produce a less studied common transcript 3' exon (region 16, exon D) (Figure 4A) as well as a potential regulatory transcript lacking a DNA bind domain and large 3' UTR (region 18, exon C5 in *fru-RA* transcript) (Usui-Aoki et al., 2000) (Figure 4A). Fru^M itself has multiple splicing isoforms that vary in the 3' end of the mRNA (fru^{MA}, fru^{MB}, fru^{MC}), which encode proteins with variable zinc finger DNA binding domain of Fru^M transcription factor (Goodwin et al., 2000; Nojima et al., 2014; Vernes, 2014). These regulate different aspects of the circuit controlling courtship behaviors, with Fru^{MC} and Fru^{MB} having the highest overlap behaviorally, and Fru^{MA} having little to no effect on courtship (Neville et al., 2014).

We previously showed that social experience and signaling from Or47b and Or67d pheromone receptors alter open chromatin marks around *fru P1* promoter in the male antennae (Zhao et al., 2020). Interestingly, examination of total transcript levels for the entire *fru* gene locus showed little to no difference across experimental conditions (Figure 1D). These small changes in total transcript levels, despite dramatic changes in open chromatin marks in wild-type SH, and mutants in *Or47b*, *Or67d,* and fru^M, prompted us to look at other aspects of gene regulation. It is known that changes in chromatin regulate many aspects of transcription such as transcriptional

232 initiation, elongation and alternative splicing (Adam and T., 2011; Naftelberg et al., 2015). The
233 effects of chromatin on splicing are thought to occur especially because chromatin state alters
234 the speed of RNA Polymerase II (RNAPII), which can lead to splicing mistakes like intron
235 retention or exon skipping (Adam and T., 2011).

236 Given the functional differences in the fru^{M} isoforms, we predicted that chromatin changes
237 caused by social experience and pheromone receptor signaling could alter *fru* splicing. To
238 explore this, we mapped reads from all experimental conditions to *fru* genomic locus and
239 investigated exon levels using DEXseq (Anders et al., 2012). In general, transcript reads from
240 *fru* locus appear noisier in experimental conditions compared to group-housed wild-type male
241 antennae, with variations in the expression of coding and non-coding sequences (Figure 4B-E).
242 In *Or47b* mutants, there is a small decrease in exon 1 (*fru P1* promoter) and male-specific exon
243 (exon 2) levels (Figure 4C; see methods – statistical analysis). *Or67d* mutants show a small
244 decrease in exon 1 levels, but male-specific exon (exon 2) is unchanged (Figure 4D). The
245 largest change in male-specific exon levels is seen in fru^{LexA}/fru^{4-40} allele (Figure 4B), which has
246 a *LexA* transgene insertion disrupting the male-specific exon and a 70-Kb deletion from the *P1*
247 promoter (Mellert et al., 2010). Exon 1 and the male-specific exon are unaltered in socially
248 isolated antennae, yet there is a small increase in the female-specific exon (exon 3) (Figure 4E).
249 In addition to the first 3 exons, a non-coding sequence (region 18) (Figure 4A), which is a part of
250 *fru-RA* transcript (Usui-Aoki et al., 2000), significantly increases in *Or67d, Or47b*, and fru^{M}
251 mutants (Figure 4C,D). This transcript encodes a Fru protein that lacks these zinc finger
252 domains but retains BTB/PDZ protein-protein interaction domain. Quantitative reverse
253 transcription PCR (qRT-PCR) experiments confirmed this finding (Figure 4-figure supplement
254 1). Increases in other untranslated regions (regions 20 and 22) are also observed in mutant
255 samples. These results suggest social and pheromonal cues alter *fru* exon usage, likely
256 indicating changes in *fru* splicing patterns.

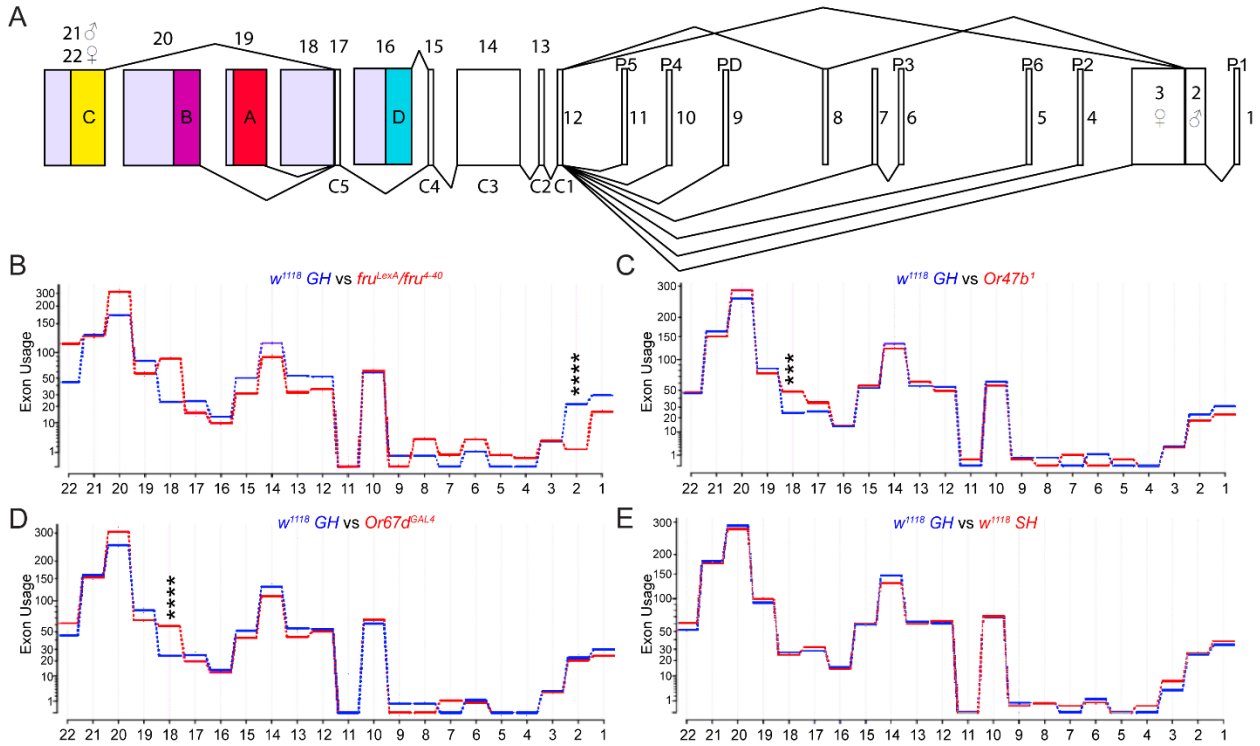

Figure 4. Olfactory stimuli regulate exon usage across the whole *fru* genomic locus. Examination of the usage of various exons in Fruitless to determine distinct changes in fru^{M} transcripts using DEXSeq. **(A)** Schematic of Fruitless: 1-22 denote each examined site. P1-P6 and PD denote promoters. C1-C5 denote common exons, while A-D denote alternatively spliced 3' DNA binding encoding domains. **(B-E)** Exon-by-exon comparison of w^{1118} *GH* vs w^{1118} *SH* **(B)**, $Or47b^{1}$ **(C)**, $Or67d^{GAL4}$ **(D)**, and $fru^{LexA}/fru^{4\text{-}40}$ **(E)**. Adjusted p-value was directly performed via DEXSeq (see methods – statistical analysis). ***, p.adjust<0.001; ****, p.adjust<0.0001. Exon 2, w^{1118} *GH* vs $fru^{LexA}/fru^{4\text{-}40}$, p.adjust=$1.25\times10^{-10}$; Exon 18 (3'UTR), w^{1118} *GH* vs $Or47b^{1}$, p.adjust=8.17×10^{-4}; Exon 18 (3'UTR), w^{1118} *GH* vs $Or67d^{GAL4}$, p.adjust=2.00×10^{-7}.

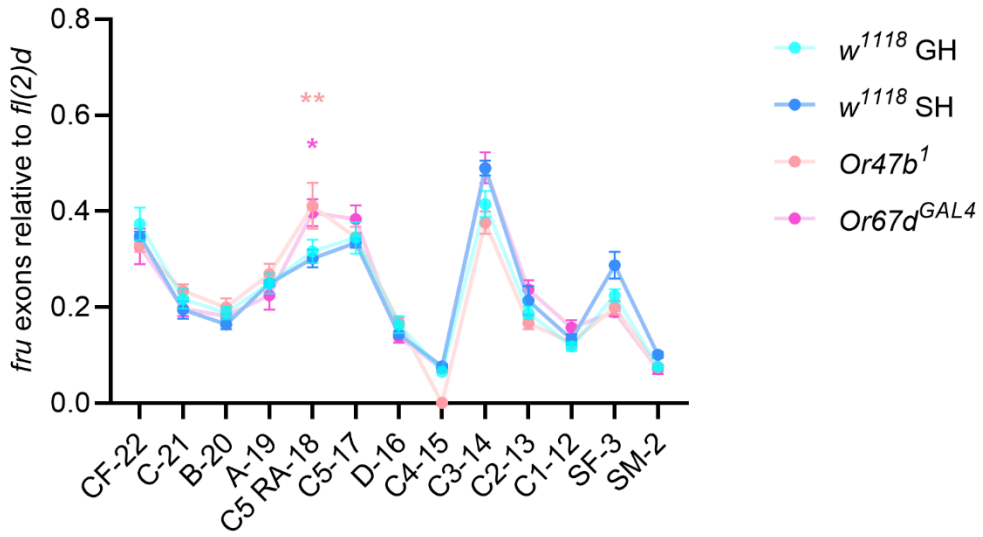

271

272 **Figure 4-figure supplement 1. Quantitative RT-PCR of *fru* exons from antennae of**

273 **group-housed and single-housed wild types, *Or47b* mutants, and *Or67d* mutants.** For

274 each genotype or condition, n = 4 biological replicates. Two-way ANOVA followed by multiple

275 comparisons within each exon (compare w^{1118} *SH*, *Or47b* mutants, and *Or67d* mutants to w^{1118}

276 *GH*). *, p<0.05; **, p<0.01. C5 RA (exon 18): $Or47b^{1}$ vs w^{1118} *GH* (p=0.0023), $Or67d^{GAL4}$ vs w^{1118}

277 *GH* (p= 0.0123).

278

279

Bimodal regulation of genes modulating neurophysiology and neurotransmission by Fru^M and pheromone receptor signaling

Previous studies have shown that pheromone receptor signaling and social experience-dependent regulation of chromatin and RNAPII enrichment around *fru P1* promoter can ultimately scale and fine-tune behavioral responses to social environment (Sethi et al., 2019; Zhao et al., 2020). Additionally, previous reports on the genome-wide binding profiles for three Fru^M isoforms in the central brain revealed isoform-specific differences in target genes that regulate neuronal development and function (Billeter et al., 2006; Neville et al., 2014). Fru^M motifs are enriched among regulatory elements that are open in the female but closed in the male, suggesting Fru^M functions as possible repressive transcription factor (Brovkina et al., 2021). Functional differences of Fru^M isoforms also influence ORN responses to their pheromone ligands (Zhang et al., 2020). Thus, chromatin-based modulation of *fru* levels and splicing with social experience and pheromone signaling can provide a quick way to modulate neuronal physiology and synaptic communication by modifying gene expression programs. Yet, the effect of social experience and pheromone receptor signaling on gene expression programs or the mode of gene regulation by Fru^M (as a transcriptional activator, repressor, or both) remains unknown.

As discussed previously, gene ontology analysis of these differentially expressed genes implies that many genes involved in neuromodulation are regulated by social context, pheromone receptor signaling, and Fru^M function. To further investigate this, we specifically zoomed into genes associated with ion channel activity and/or neurotransmitter regulation (Figure 5A,B; Figure 6A,B). We clustered these genes based on their log_2 fold change in transcript levels compared to group-housed wild types in each experimental condition, while also showing their

304 corresponding expression levels in the antennae (RPKM, reads per kilobase of transcript, per
305 million mapped reads) (Figure 5A,B; Figure 6A,B). We found many ion channel and/or
306 neurotransmitter receptor-encoding genes showed up/down-regulation in response to social
307 isolation, and loss of Or47b, Or67d, or Fru^M function (Figure 5A,B; Figure 6A,B). Within ion
308 channels, two subclasses stand out. These are the Degenerin/Epithelial Sodium Channel
309 (DEG/ENaC) proteins known as pickpockets (ppks) and inward-rectifying potassium channels
310 Irks. Additional genes also include those encoding calcium channels, for example, *Piezo*, *TrpA1*,
311 and *cacophony* (*cac)* (Figure 5A,B).

312

313 *ppk gene family*

314 Recent reports pointed to the function of DEG/ENaC channels known as *pickpocket* family of
315 sodium channels that act in Or47b and Or67d ORNs to regulate responses to their ligands
316 (Zhang et al., 2020). Fru^M binding motifs have been identified around many of these *ppk* family
317 members, such as *ppk*, *ppk5*, *ppk6, ppk15, ppk19*, *ppk23*, *ppk25,* and *ppk30* (Dalton et al.,
318 2013; Neville et al., 2014; Vernes, 2014). Both *ppk23* and *ppk25* have been identified as
319 necessary for changes of physiology in Or47b ORNs through Fru^{MB} and Fru^{MC} activity,
320 respectively, with Fru^{MB} having an antagonistic effect on physiology in Or67d ORNs (Zhang et
321 al., 2020). We therefore first examined the expression levels of *ppk* genes in the antennae. In
322 group-housed wild-type antennae, *ppks* show varying degrees of and generally low expression,
323 with *ppk5* displaying the highest levels (Figure 5C). Many *ppk* genes, including *ppk23,* seem not
324 to be expressed in antenna. Analysis of recent single-cell RNA-seq data from ORNs (Li et al.,
325 2020) revealing ORN class-specific expression of *ppk*s also agree with this pattern, though a
326 few *ppks* known to be expressed in several ORN classes are not detectable in this dataset,
327 possibly due to the limitations of single-cell RNA-seq in detecting low-abundance genes (Figure
328 5-figure supplement 1A). Even though there is no effect on the expression of any *ppk* family

329 members in socially isolated male antennae, many *ppk* genes are differentially regulated in *fru*^{M}
330 mutants, in agreement with the existing Fru^{M} binding sites at their promoters. For example*, ppk6*
331 *and ppk25* are upregulated in *fru*^{M} mutants whereas *ppk5*,*7*,*13*,*14*,*15*,*19* are downregulated.
332 Many of these genes also show correlated changes in *Or47b* and/or *Or67d* mutants
333 (*ppk13*,*14*,*15*,*19*,*25*). *ppk6* is strikingly upregulated in both *fru*^{M} and *Or67d* mutants, whereas
334 *ppk7* is downregulated in both *Or47b* and *fru*^{M} mutants (Figure 5C'). Of note is the significant
335 changes in *ppk25* expression as *ppk25* has been found to change the sensitivity of Or47b
336 neurons, is expressed in Or47b and Ir84 ORNs, but not Or67d ORNs, and has recently been
337 shown to be downstream of Or47b and Ir84a activity (Ng et al., 2019; Pikielny, 2012) (Figure
338 5C). The changes in *ppk25* levels were also validated through quantitative RT-PCR (Figure 5-
339 figure supplement 1C-E). The bimodal changes in *ppk* transcripts in *fru*^{M} mutants suggest Fru^{M}
340 can act as both a repressor and an activator of *ppk* gene regulation. Furthermore, given that
341 pheromone receptor function regulates Fru, the patterns of *ppk* gene misregulation in *Or47b*
342 and *Or67d* mutants are likely dependent on changes in Fru^{M} activity downstream of pheromone
343 receptor signaling.

344

345 *Irk gene family*

346 Irk gene family encodes 3 inwardly rectifying potassium channels (Irk1-3) with binding motifs for
347 Fru^{MA} identified upstream of *Irk2* and binding of both Fru^{MA} and Fru^{MC} found around *Irk3* (Dalton
348 et al., 2013; Neville et al., 2014; Vernes, 2014). Three *Irk* genes are expressed in varying levels
349 in the antennae with *Irk1* having the lowest expression and *Irk2* having the highest expression
350 (Figure 5D). We found that *Irk1* is upregulated in *Or47b* mutants, whereas *Irk2* shows the trend
351 towards upregulation in response to social isolation (Figure 5D').

352 These results suggest that changes in the transcript levels of Fru^M regulated sodium and
353 potassium channels with social isolation and in pheromone receptor mutants may contribute to
354 changes in neuronal responses and behaviors.

355

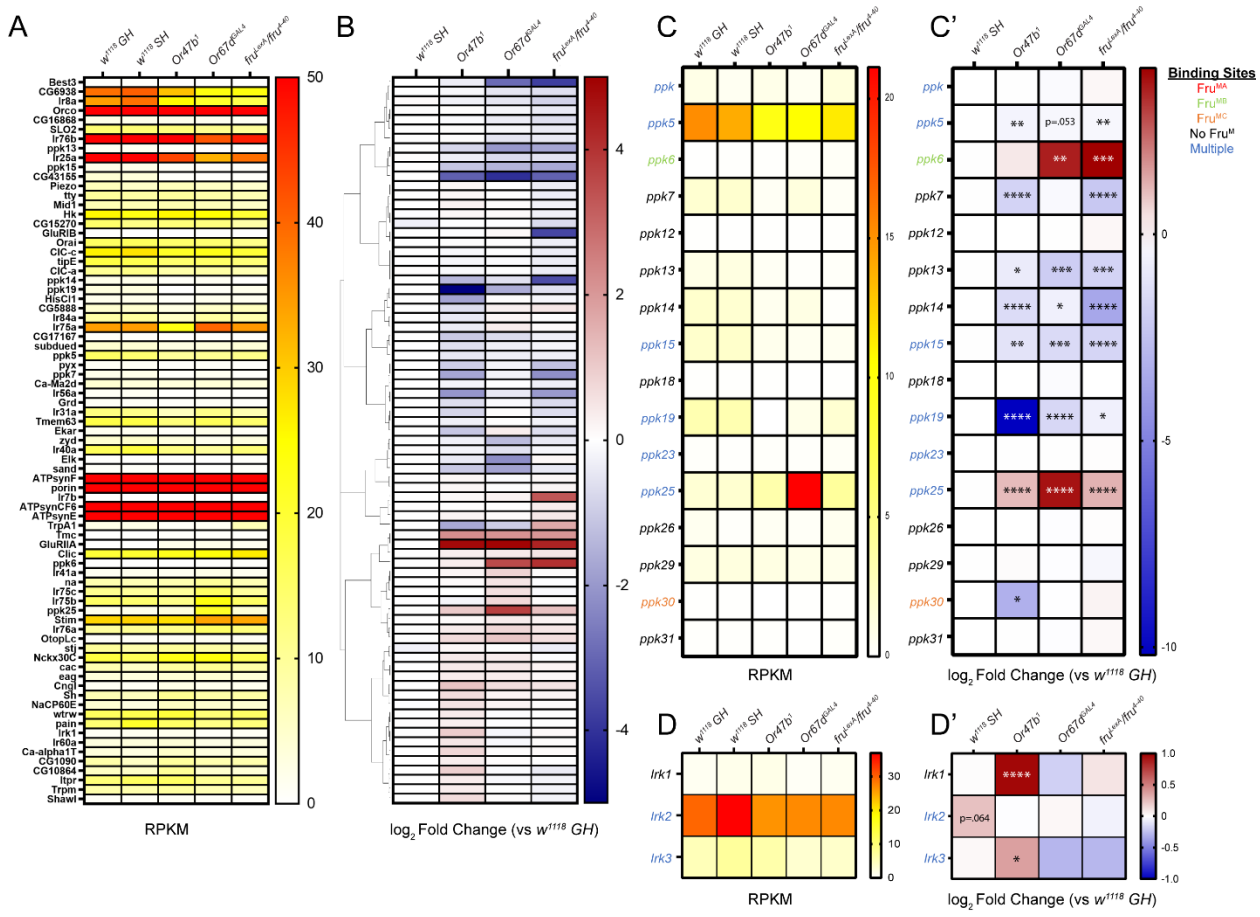

Figure 5. Differentially expressed ion channel-encoding genes in response to social isolation and loss of pheromone receptors or *fru*^{M}. (A-B) Examination of GO term: 0005216 (ion channel activity) shows significant changes in various ion channel subclasses. Hierarchically clustered heatmaps showing $\log_2$ fold change compared to group-housed wild-type antennae across all experimental conditions **(B)** and average mRNA levels (RPKM) of replicates within each condition ordered in the same way as $\log_2$ fold change **(A)**. Genes that are not significant (adjusted p-value above 0.01) in any experimental condition were filtered out. **(C-C')** RPKM **(C)** and $\log_2$ fold change **(C')** for *pickpocket* (*ppk*) gene family. **(D-D')** RPKM **(D)** and $\log_2$ fold change **(D')** for *inwardly rectifying potassium channel* (*Irk*) gene family. Adjusted p-value was directly performed

368 via DESeq2. *, p.adjust<0.05; **, p.adjust<0.01; ***, p.adjust<0.001; ****,

369 p.adjust<0.0001.

370

371

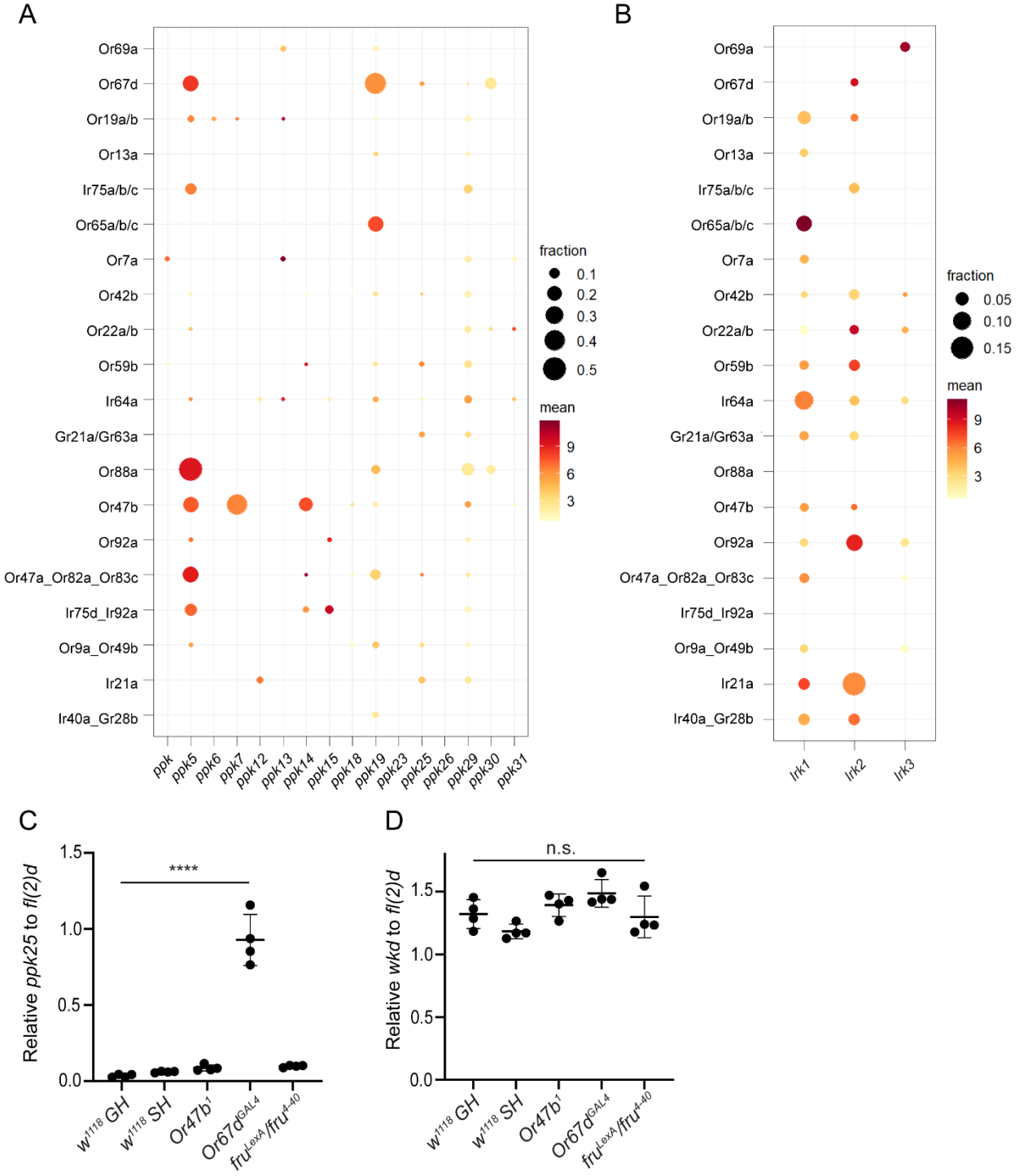

Figure 5-figure supplement 1. Validation of *ppk* expression across ORN classes and in mutants. (A-B) ORN class-specific expression of *ppk* and *Irk* family genes based on single-cell RNA-seq datasets from the adult ORNs (McLaughlin et al., 2021).

377 Size of each circle indicates the fraction of positive cells (log_2(CPM+1)>0.5) and color
378 intensity indicates the mean expression (log_2(CPM+1)) of all positive cells. **(C-D)**
379 Quantitative RT-PCR validation of *ppk25* expression (C) and a negative control gene
380 *wkd* expression (D) from antennae of grouped and socially isolated wild types, *Or47b*
381 mutants, *Or67d* mutants, and fru^M mutants normalized to *fl(2)d*. *fl(2)d* and *wkd* were
382 selected based on their near-identical expression level across all conditions from the
383 RNA-seq results and thus used as loading and negative control genes. For each
384 genotype or condition, n=4 biological replicates. One-way ANOVA followed by multiple
385 comparisons (compare other groups to group-housed wild types w^{1118} *GH*). ****,
386 p<0.0001.

387

388

389 *Regulators of Neurotransmission*

390 To ask if social experience, pheromone signaling, and Fru^M function regulate genes involved in
391 neurotransmission, we next examined the expression of neurotransmitter receptors,
392 transporters, and synthesizers. ORNs in the antennae are mostly cholinergic (Wilson, 2013). In
393 the antennal lobe it has been shown that lateral neurons, which include serotonergic,
394 GABAergic, and glutamatergic interneurons, provide cross talk between antennal lobe neurons
395 (Chou et al., 2010; Wilson, 2013). These neurons form connections on the presynaptic bouton
396 of ORN synapses to cause lateral excitation or inhibition across glomeruli (Olsen et al., 2007;
397 Wang et al., 2003; Wilson, 2013). These connections are required for fine tuning of signaling at
398 synapses as a way of rapid modulation of neuronal function (Dacks et al., 2009; Johnson et al.,
399 2009; Mohamed et al., 2019; Olsen et al., 2007; Sizemore and Dacks, 2016; Sudhakaran et al.,
400 2012; Suzuki et al., 2020; Wang et al., 2003; Wong et al., 2002; Zhang et al., 2019). We found a
401 high expression of choline acetyltransferase (*ChAT*) that catalyzes acetylcholine biosynthesis
402 and *VAChT* that packages acetylcholine into synaptic vesicles, coinciding with their reported
403 cholinergic roles. Moreover, we also found relatively high expression of several genes encoding
404 receptors of various neurotransmitters, such as choline, serotonin (5-HT), GABA, and glutamate
405 (Figure 6C-F'). Many of these genes, such as *nAChRalpha4*/*5*, *5-HT2A*, *5-HT7*, *GABA-B-R2*,
406 and *GluRIIA*, have previously been found to regulate courtship behavior in flies through
407 signaling in the antennal lobe (Becnel et al., 2011; Clowney et al., 2015; Johnson et al., 2011;
408 Suzuki et al., 2020). Interestingly, *GABA-B-R2* was shown to be specifically involved in
409 presynaptic gain control of Or47b ORNs (Root et al., 2008). Additionally, single-cell RNA-seq
410 data shows both broadly expressed neurotransmitter genes like *GluRIIB* and 5-*HT2B*, while
411 others are specific to a subset of ORN classes (McLaughlin et al., 2021) (Figure 6-figure
412 supplement 1). Overall, many of the genes encoding neurotransmitter receptors show
413 expression changes in different experimental conditions (Figure 6B).

414 To zoom into genes related to specific neurotransmitters, we didn't observe any significant
415 changes in response to social isolation, though a few genes, like *dmGlut,* appear to be
416 upregulated compared to the grouping condition (Figure 6C,D'). We again found that loss of
417 Fru^M function led to bimodal effects on gene expression (Figure 6C-F'). Indeed, many of these
418 genes have known Fru^M binding to their promoters, including receptors *nAChRalpha1*/*3*/*4*/*5,*
419 G*luRIIA*, *GluClalpha*, *5-HT1A*, *5-HT1B*, *5-HT2A*, *5-HT7*, and transporters/regulators such as
420 *VAChT, ChAT*, and *Gat* (Dalton et al., 2013; Neville et al., 2014; Vernes, 2014). Some of these
421 genes display correlated changes between pheromone receptor mutants and fru^M mutants, like
422 *GluRIIA*, *dmGlut*, and *5-HT2A*, suggesting that the effects of pheromone signaling on
423 neurotransmission can act via their influences on *fru* regulation (Figure 6D-E'). The changes in
424 *5-HT2A* were also validated through qRT-PCR (Figure 6-figure supplement 2). Evident changes
425 are also observed in some genes not known to be Fru^M targets, for example, *GluRIB* which
426 shows downregulation only in fru^M mutants, and *5-HT2B* which shows upregulation in *Or47b*
427 and fru^M mutants (Figure 6D-E'). These may reflect effects of pheromone receptor signaling
428 independent of Fru^M function or indirect effects of Fru^M activity. To summarize, the systems-level
429 changes in expression of genes involved in neurotransmission and neurophysiology with social
430 experience and pheromone receptor signaling can modulate ORN responses. In addition, these
431 effects on gene expression with social signals can occur either in a Fru^M-dependent manner or
432 independently of Fru^M in response to other gene regulatory pathways activated by pheromone
433 receptor signaling.

434

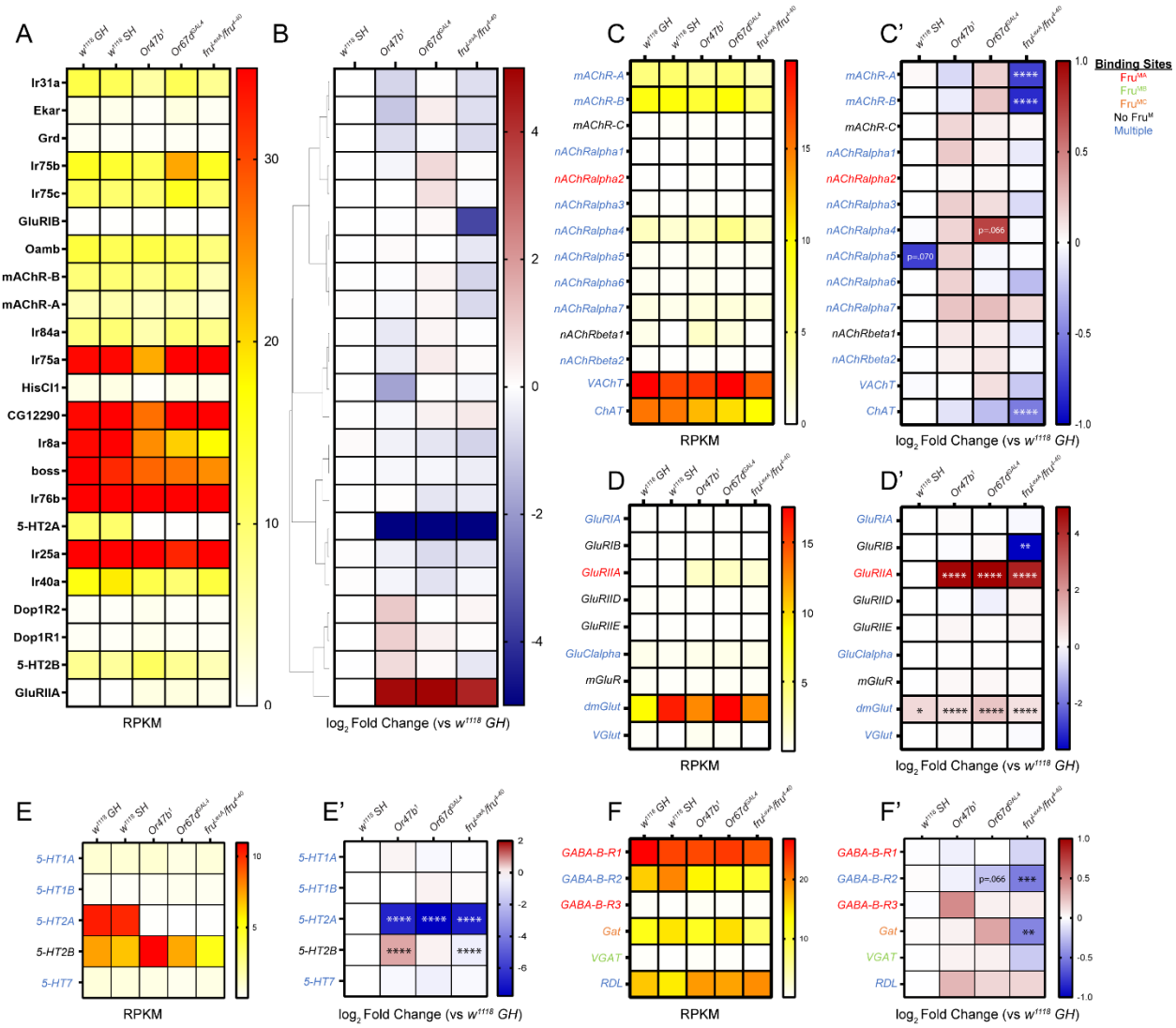

Figure 6. Differentially expressed neurotransmitter receptor and transporter-encoding genes in response to social isolation and loss of pheromone receptors or *fru*^{M}. (A-B) Examination of GO term: 0030594 (neurotransmitter receptor activity) shows significant changes in various neurotransmitter activity-associated subclasses. Hierarchically clustered heatmaps showing $\log_2$ fold change compared to group-housed wild-type antennae across all experimental conditions **(B)** and average mRNA levels (RPKM) of replicates within each condition ordered in the same way as $\log_2$ fold change **(A)**. Genes that are not significant (adjusted p-value above 0.01) in any experimental

445 condition were filtered out. **(C-C')** RPKM **(C)** and log_2 fold change **(C')** for acetylcholine-
446 associated genes. **(D-D')** RPKM **(D)** and log_2 fold change **(D')** for glutamate-associated
447 genes. **(E-E')** RPKM **(E)** and log_2 fold change **(E')** for serotonin-associated genes. **(F-F')**
448 RPKM **(F)** and log_2 fold change **(F')** for GABA-associated genes. Adjusted p-value was
449 directly performed via DESeq2. *, p.adjust<0.05; **, p.adjust<0.01; ***, p.adjust<0.001;
450 ****, p.adjust<0.0001.

451

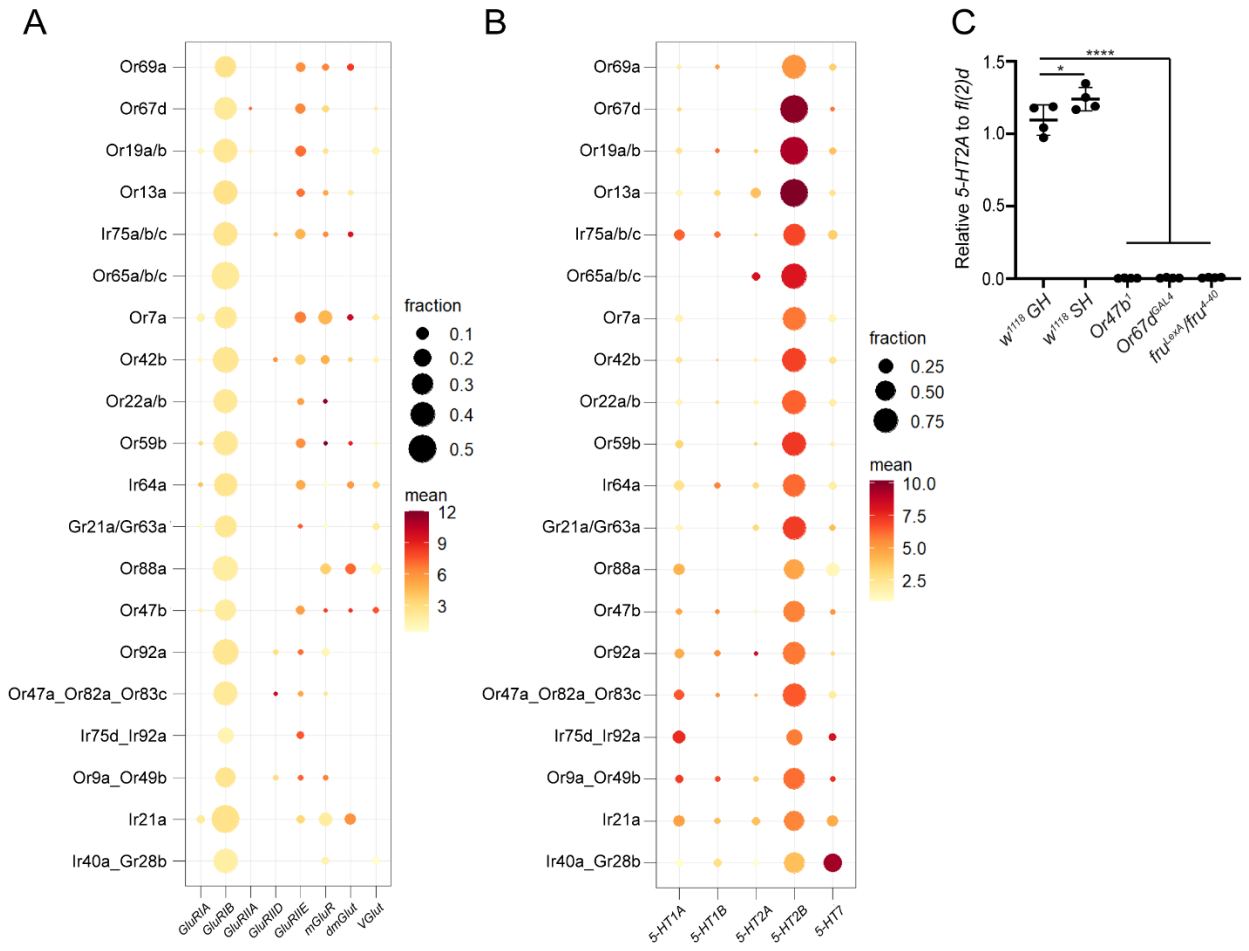

Figure 6-figure supplement 1. Validation of neurotransmitter receptor expression across ORN classes and in mutants. (A-B) ORN class-specific expression of serotonin and glutamate receptors based on single-cell RNA-seq datasets from the adult ORNs (McLaughlin et al., 2021)**.** The size of each circle indicates the fraction of positive cells ($\log_2$(CPM+1)>0.5) and color intensity indicates the mean expression ($\log_2$(CPM+1)) of all positive cells. **(C)** Quantitative RT-PCR validation of *5-HT2A* expression. Relative expression of *5-HT2A* from antennae of grouped and socially isolated wild types, *Or47b* mutants, *Or67d* mutants, and fru^M mutants normalized to *fl(2)d*. For each genotype or condition, n=4 biological replicates. One-way ANOVA

463 followed by multiple comparisons (compare other groups to group-housed wild types

464 w^{1118} *GH*). *, $p<0.05$; ****, $p<0.0001$.

465

466

Pheromone receptor signaling regulates genes involved in hormone metabolism

Previous studies have identified age-related cues such as juvenile hormone (JH) signaling together with social experience to control Or47b neuronal responses to pheromones and courtship behaviors in a Fru^{M}-dependent manner (Lin et al., 2016; Sethi et al., 2019; Zhang and Su, 2020). JH signaling, concurrent with social experience, modifies chromatin around *fru P1* promoter and ultimately fru^{M} levels in Or47b ORNs (Zhao et al., 2020). These studies also demonstrated that JH receptor enrichment at *fru P1* promoter increases in socially isolated flies as well as flies with disrupted Or47b signaling (Zhao et al., 2020). As mentioned above, gene ontology analysis in this study also brings genes involved in hormone metabolism (Figure 3). Thus, we specifically interrogated the genes regulating juvenile hormone levels in pheromone receptor and fru^{M} mutants (Figure 7A-C').

Many of the enzymes involved in juvenile hormone biosynthesis and metabolism, such as juvenile hormone epoxide hydrolases (*Jheh1*,*2*,*3*), juvenile hormone esterase (*Jhe*), and juvenile hormone acid methyltransferase (*jhamt*), are expressed at varying levels in the antennae (Figure 7C; Figure 7-figure supplement 1). These genes are also reported to have Fru^{MA} and Fru^{MC} binding in their upstream regulatory elements (Dalton et al., 2013; Neville et al., 2014; Vernes, 2014). Two mostly enriched genes, *Jheh1* and *Jheh2*, show mild upregulation in fru^{M} mutants but no significant changes in the absence of social cue or pheromone receptor signaling (Figure 7C,C'). On the other hand, both *Jhe* and *Jheh3* appear to be upregulated in social isolation while downregulated in *Or47b* mutants (Figure 7C'; Figure 7- figure supplement 1). *Jhe* is of particular interest as Jhe activity is known to be necessary for robust male-specific courtship behaviors and mating success in addition to affecting the abundance of sex-specific pheromones such as 11-cis-vaccenyl acetate in males (Ellis and Carney, 2010; Liu et al., 2008). Furthermore, seminal work on Jhe and Jheh3 has shown that these enzymes work together to

492 catabolize JH in *D. melanogaster* (Khlebodarova et al., 1996). These results suggest that social
493 experience and pheromone receptor signaling regulates the expression of JH biosynthetic
494 enzymes. Such changes can modulate juvenile hormone activity by rapidly catabolizing JH in
495 the periphery and affecting downstream target genes, such as *fruitless*.

496

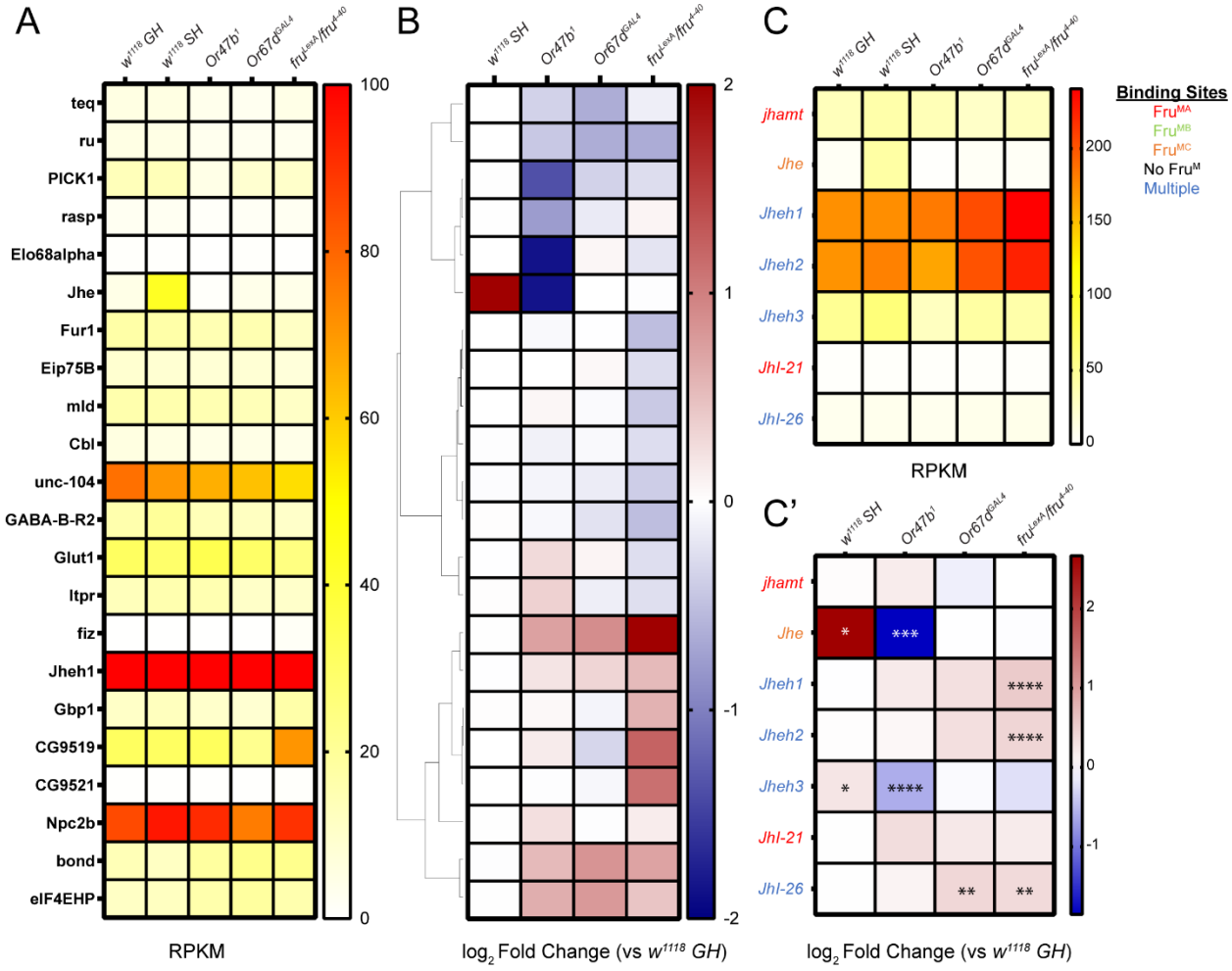

Figure 7. Differentially expressed hormone regulator-encoding genes in response to social isolation and loss of pheromone receptor or *fru*^{M}. (A-B) Examination of GO term: 0010817 (regulation of hormone levels) shows significant changes in various hormone regulation-related gene subclasses. Hierarchically clustered heatmaps showing $\log_2$ fold change compared to group-housed wild-type antennae across all experimental conditions **(B)** and average mRNA levels (RPKM) of replicates within each condition ordered in the same way as $\log_2$ fold change **(A)**. Genes that are not significant (adjusted p-value above 0.01) in any experimental condition were filtered out.

507 **(C-C')** RPKM **(C)** and log_2 fold change **(C')** for juvenile hormone metabolism-related

508 genes. Adjusted p-value was directly performed via DESeq2. *, p.adjust<0.05; **,

509 p.adjust<0.01; ***, p.adjust<0.001; ****, p.adjust<0.0001.

510

511

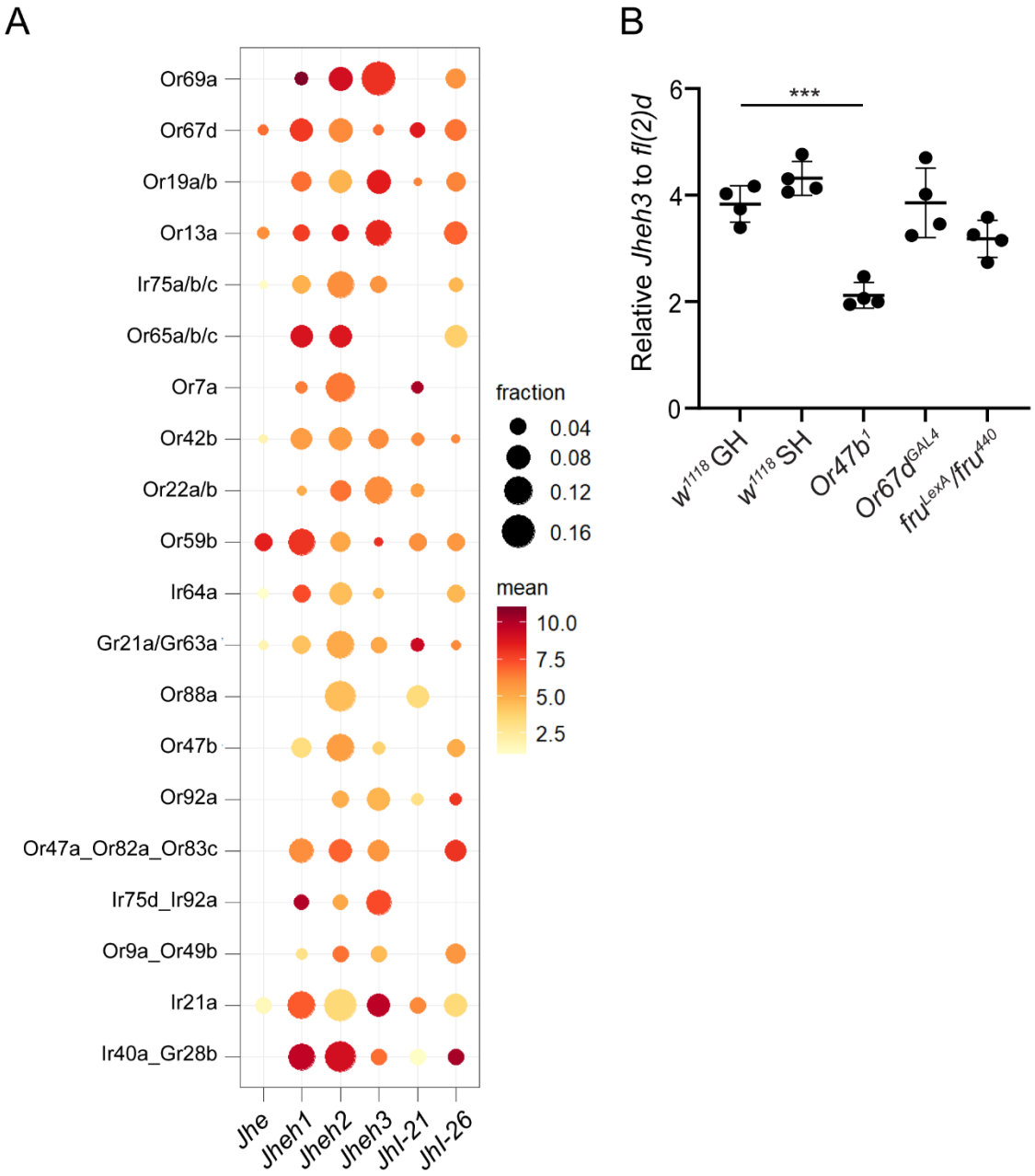

512

513 **Figure 7--figure supplement 1. Validation of hormone-related gene expression**

514 **across ORN classes and in mutants. (A-B)** ORN class-specific expression of juvenile

515 hormone regulators based on single-cell RNA-seq datasets from the adult ORNs

516 (McLaughlin et al., 2021)**.** The size of each circle indicates the fraction of positive cells

517 (log_2(CPM+1)>0.5) and color intensity indicates the mean expression (log_2(CPM+1)) of

518 all positive cells. **(C)** Quantitative RT-PCR validation of *Jheh3* expression. Relative
519 expression of *Jheh3* from antennae of grouped and socially isolated wild types, *Or47b*
520 mutants, *Or67d* mutants, and fru^{M} mutants normalized to *fl(2)d*. For each genotype or
521 condition, n=4 biological replicates. One-way ANOVA followed by multiple comparisons
522 (compare other groups to group-housed wild types w^{1118} *GH*). ***, $p<0.001$.

523 # Discussion

524 Sensory experience influences many behaviors by modifying neural circuit function (Curley et
525 al., 2011; Cushing and Kramer, 2005; Dey et al., 2015; Sethi et al., 2019). Yet, sensory
526 experience-dependent molecular mechanisms that adjust circuit function and behaviors to the
527 environment remain largely unknown. Here, we took advantage of the well-characterized and
528 defined system of sex-specific behaviors, governed by the Fru^M, which acts as a gene
529 regulatory switch for male-specific circuit development, function, and behavior in *Drosophila*
530 *melanogaster* (Dickson, 2008; Yamamoto, 2007; Yamamoto and Koganezawa, 2013;
531 Yamamoto and Kohatsu, 2017). Our results show that social experience and pheromone
532 signaling alters Fru^M splicing patterns and neuromodulatory gene expression programs, which
533 ultimately modulate circuit function and behavioral responses.

534 Previous studies demonstrated that social experience can modulate Fru^M-dependent sex-
535 specific behaviors such as courtship and aggression (Curley et al., 2011; Dey et al., 2015; Sethi
536 et al., 2019). For example, social isolation decreases the sensitivity of Or47b neurons to their
537 pheromone ligands in a Fru^M-dependent manner, which leads to a decrease in male competitive
538 courtship advantage (Sethi et al., 2019). Other studies have also shown that monosexual group
539 housing can decrease the manifestation aspects of courtship behaviors such as courtship song
540 and circling (Dankert et al., 2009). In addition to courtship, aggression behaviors which are
541 under the control of Or67d and Or65a neurons and Fru^M function, also change with social
542 experience (Dankert et al., 2009; Liu et al., 2011). For example, social isolation significantly
543 increases male-male aggression (Dankert et al., 2009; Wang et al., 2008). These reports
544 highlight the importance of social experience and pheromone signaling in the execution of sex-
545 specific behaviors.

546 What are the molecular mechanisms by which Fru^M function is altered by social experience? We
547 previously reported that social experience and Or47b signaling alters chromatin states around
548 *fru* P1 promoter (Zhao et al., 2020). These chromatin changes around *fru* with pheromone
549 signaling and social experience modifies the levels of fru^M transcripts (Hueston et al., 2016;
550 Sethi et al., 2019; Zhao et al., 2020). Nonetheless, the consequential details of chromatin-based
551 changes on *fru* transcription remained unknown. One of our most intriguing findings from this
552 transcriptome analysis is that these chromatin effects are associated with changes in the
553 relative exon usage and splicing patterns of *fru* gene in response to impaired pheromone
554 detection (Figure 4). Transcriptional regulation of *fru* is complex yielding 15 annotated
555 alternatively spliced isoforms from 7 promoters giving rise to different 3' sequences which
556 encode Zinc-finger DNA-binding domains of Fru protein (Lee et al., 2000; Meier et al., 2013;
557 Nojima et al., 2014; Von Philipsborn et al., 2014). Alternative splicing generates Fru proteins
558 with slightly different DNA-binding properties upstream of target genes which can have binding
559 sites for single or multiple Fru^M isoforms (Dalton et al., 2013; Neville et al., 2014; Vernes, 2014).
560 Many of these genes encode regulators of neural development and function. Therefore,
561 changes in *fru* splicing patterns can affect the expression of thousands of genes simultaneously,
562 strongly modulating neuronal responses and circuit outputs in a short period of time.
563 Remarkably, Fru^M is expressed in ~2000 interconnected neurons highlighting a circuit for
564 courtship behaviors from sensation to action with expression (Sato and Yamamoto, 2020;
565 Yamamoto and Koganezawa, 2013). This expression pattern allows such neural activity-
566 dependent influences on *fru* chromatin and transcription to propagate throughout the whole
567 circuit. In summary, these features make circuit switch gene fru^M an efficient molecular hub onto
568 which many internal and external factors may act to modulate circuit activity and behavioral
569 outputs by tweaking the levels of transcripts and splicing isoforms, leading to cascade changes
570 in transcriptional programs.

571 Each pheromone sensing circuit relays different information about the social environment, which
572 is integrated and processed to output a specific behavior. Likely due to differences in neuronal
573 identity and function, different pheromone receptors have different effects on *fru* chromatin and
574 splicing isoforms (Zhao et al., 2020)(Figure 4). Such sensory stimuli-dependent changes in Fru
575 proteins can alter the expression of downstream neuromodulatory genes to have rapid,
576 temporary, or lasting effects on neuronal activity and behavioral outputs. These changes are
577 essential for organisms to form short/long-term adaptation to the environment. However, how
578 these different cell types generate these differences in behavioral repertoire via changes in
579 gene expression in the periphery have been largely unknown.

580 Many of the genes that show differential expression in response to social isolation and
581 disruption of pheromone receptor or Fru^M function encode neuromodulators that affect
582 membrane potential, such as ion channels, transporters, and neurotransmitter receptors (Figure
583 3; Figure 5; Figure 6). Among all conditions, social isolation possesses the fewest differentially
584 expressed genes compared to group-housed controls with a small overlap with pheromone
585 receptor and fru^M mutants. This might be due to differences in gene expression changes in
586 response to disruption of spontaneous activity of pheromone sensing olfactory neurons with
587 socially isolation versus disruption of both spontaneous and evoked activity in pheromone
588 receptor mutants. Loss of Fru^M alters the expression of many neuromodulatory genes with
589 known Fru^M binding sites in a bimodal way, suggesting Fru^M can act as both an activator and
590 repressor of gene expression. Some of these differentially expressed genes are also altered in
591 pheromone receptor mutants, generally in the same direction (Figure 2D,E). There are also
592 unique overlaps between *Or47b* and fru^M mutants, between *Or67d* and fru^M mutants, and
593 between *Or47b* and *Or67d* mutants (Figure 2B,E). Many of these differentially expressed genes
594 are known to harbor binding sites for different Fru^M isoforms. These suggest that some of the

595 differentially expressed genes in *Or47b* and *Or67d* mutant are due to Fru^{M}-dependent changes,
596 whereas others might be Fru^{M}-independent, caused by OR signaling and/or ORN activity.

597 One functionally relevant gene among the genes that show differential regulation in pheromone
598 receptor and *fru^{M}* mutants is the Fru^{M} target gene *ppk25*, which previously was shown to
599 modulate ORN responses in Or47b and Or67d neurons (Ng et al., 2019; Zhang et al.,
600 2020). *ppk25* belongs to a family of sodium channels that serve a variety of functions, from
601 neuromodulation to detection of sensory cues. PPK protein complexes, generally are composed
602 of multiple subunits encoded by different *ppk* genes. Many *ppk* genes contain binding sites for
603 Fru^{M} isoforms in their promoter regions (Dalton et al., 2013; Neville et al., 2014; Vernes, 2014).
604 In addition, a recent study implicated isoform-specific Fru^{M}-dependent regulation of *ppk25* and
605 *ppk23* in the modulation of Or47b and Or67d responses (Ng et al., 2019; Zhang et al., 2020).
606 According to the genetic analysis in this study, Fru^{MB} and Fru^{MC} positively regulate the
607 expression of *ppk25* and *ppk23*, respectively. There are apparent discrepancies with this
608 interpretation and transcriptome data from our study, as well as others (Li et al., 2020;
609 McLaughlin et al., 2021). While our transcriptome analysis agrees with a regulatory role for Fru^{M}
610 in *ppk25* gene regulation, the regulatory mode is repressive; that is, *ppk25* expression is
611 upregulated in *Or47b*, *Or67d,* and *fru* mutants. This type of repressive role for Fru^{M} in
612 transcription also is in consensus with previous studies demonstrating Fru^{M} interactions with
613 transcriptionally repressive histone-modifying enzymes such as HDAC1 (Ito et al., 2013, 2012).
614 In addition, we are not able to detect any transcripts for *ppk23* in the antennae, and the
615 expression of *ppk23* does not change in *Or47b*, *Or67d,* and *fru^{M}* mutants. Instead, we noticed
616 other *ppk* genes such as *ppk6*,*7*,*13*,*14*,*15*,*19* are altered in different mutant conditions. Fru^{M}
617 seems to have a bidirectional role in regulating *ppk* gene expression, where it activates the
618 expression of a subset of *ppk* genes (*ppk7*,*13*,*14*,*15*) while repressing the expression of others
619 (*ppk6* and *ppk25*). One way to reconcile these differences is that multiprotein PPK complexes

620 composed of combinations of different PPK subunits, and the stoichiometric levels of each *ppk*
621 transcript in a given neuron can determine channel function. For example, misexpression of
622 *ppk23*, which normally is not expressed in the antennal ORNs, can interfere with PPK channel
623 function by disrupting the existing functional complexes in a given neuron or forming new PPK
624 complexes, thus affecting physiological properties. Another possibility is that the slight
625 upregulation of *ppk25* in *Or47b* and fru^M mutants as well as large changes in *Or67d* mutants
626 may be due to global fru^M changes in the whole antennae, or through retrograde
627 neuromodulatory signaling from the antennal lobe.
628 Antennal sensilla contain cell types other than ORNs, such as glia-like cells and support cells of
629 sensillum, as well as epithelial cells. Since our transcription data is from the whole antennae,
630 one possibility we cannot exclude is that differences in antennal gene expression in different
631 genetic and social conditions are readouts from non-neuronal cells. Even though we anticipate
632 the immediate effects of *Or67d* and *Or47b* mutants to happen in the ORNs expressing these
633 two receptors, signals from ORNs can lead to secondary changes in gene expression in non-
634 neuronal cells within the sensillum. This also brings to light a general issue with bulk tissue and
635 whole gene knockouts where large cell-type-specific changes may be masked by cell-
636 nonautonomous changes in gene expression from others cell types, as well as retrograde
637 feedback signaling within olfactory circuits. Regardless, our data shows many of the
638 differentially expressed genes encode regulators of neuronal function and neuromodulation.
639 This increases the likelihood that the transcriptional changes in response to social and
640 pheromonal cues are happening mostly in the neurons that respond to social cues, such as
641 Or47b and Or67d ORNs. Future single-cell chromatin and transcription profiles from Fru^M-
642 positive neurons in the antenna and brain will provide deeper insights to neuron-specific
643 changes in gene regulation from the peripheral to the central nervous system that modulate
644 circuit function in response to social cues.

Material and Methods

Fly genetics and genotypes

Flies were raised on standard fly food (containing yeast, cornmeal, agar, and molasses) at 25°C in a 12-hour light/12-hour dark cycle in cylindrical plastic vials (diameter, 24 mm and height, 94 mm). For social isolation (single housing, SH) condition, 80-100 hour-old pupae were separated by sex and males were placed into individual vials, allowed to eclose alone, and aged to 7 days to deprive flies of pheromone interaction on ORNs. For group housing (GH) condition, 25-30 newly eclosed males were collected and placed into food vials. These were aged to 7 days and 180 antennae were dissected per sample, for a total of 3 samples for w^{1118} *GH*, 3 samples for w^{1118} *SH*, 3 samples for $Or47b^{1}$ mutants (*$Or47b^{1}$/$Or47b^{1}$; Or47b-GAL4, UAS-mCD8GFP/ Or47b-GAL4, UAS-mCD8GFP*), 3 samples for $Or67d^{GAL4}$ mutants (*UAS-mCD8GFP/ UAS-mCD8GFP; $Or67d^{GAL4}$/$Or67d^{GAL4}$*), and 2 samples for fru^{LexA}/ fru^{4-40} mutants (*w^{+}; +/+; fru^{LexA}/ fru^{4-40}*). All fly strains w^{1118}, $Or67d^{Gal4}$, $Or47b^{1}$, fru^{lexA}/fru^{4-40}, were maintained at room temperature.

RNA-seq

RNA-seq was performed as described before (Li et al., 2016). Male flies are aged for 7 days and dissected for the third antennal segment (~180 antennae per genotype). RNA was extracted from dissected tissues samples using Qiagen RNA-easy extraction kit, quantified using a Qubit RNA assay kit and checked for quality using a High Sensitivity RNA ScreenTape on a TapesStation (Agilent). RNA integrity scores are typically 7.0 and greater. 1ug of RNA was used to construct libraries for sequencing using a KAPA mRNA library prep kit with polyA RNA selection. Barcoded libraries are sequenced on a Novaseq 6000 SP 50 bp following manufacturer's instructions (Illumina). After demultiplexing sequence quality was assessed using FASTQC (Version 0.11.9). While there are issues with under-clustering of the samples

668 and unbalanced pools, the data quality was typical for RNA extracted from fresh frozen material.
669 The unbalanced pools resulted in differences in sequencing depth of each sample.

670 Analysis of RNA-seq data

671 Once sequenced, the reads are preprocessed with FASTP (S. Chen et al. 2018) to remove
672 adaptors and trim/filter for quality. These are mapped to the dm6 reference genome using
673 MapSplice2 (Wang et al. 2010), with individual mapping rates exceeding 98% in all cases. This
674 raw alignment was deduplicated and filtered for mapping quality and correct pairing; additional
675 alignments are generated to confirm results are robust to mapping ambiguity. Mapped reads are
676 assigned to genes in the annotation using the feature Counts command from the SubRead
677 package (Liao, Smyth, and Shi 2014). Differential expression was modeled using DESeq2
678 (Love, Huber, and Anders 2014) using the “apeglm” shrinkage estimator, and data was
679 processed and visualized in R using the tidyverse framework (Wickham et al 2019),
680 supplemented with the biomaRt (Durinck et al 2009), ComplexHeatmap (Gu, Eils, & Schlesner,
681 2016) and UpSet (N. Gehlenborg 2019) packages. The bioinformatics pipeline was
682 implemented in Snakemake (Köster, J., & Rahmann, S. 2012). Code for the analysis is
683 deposited on GitHub
684 (https://github.com/csoeder/VolkanLab_BehaviorGenetics/tree/master/scripts).

685 DEXSeq was used to test for differential exon use under models corresponding to those used in
686 differential gene expression (Anders et al., 2012). From the genome-wide test, the *fruitless*
687 locus was examined in particular. Further post-hoc t-tests are processed on non-normalized
688 data of individual read count comparisons to look for differences at individual exons.

689 Statistical analysis

690 Adjusted p-value were directly calculated from DESeq2 or DEXSeq. Other statistical analysis is
691 described in the legend of corresponding figures.

692 Specifically, to compare the exon usage in Figure 4, we also calculated p-value from t-tests of
693 independent comparisons of group housed male antennae transcriptome to each experimental
694 condition at an individual exon segment (1-22, see the table below). Even though many exons
695 level differences were significant using this method, adjusted p-value from DEXSeq gave rise to
696 fewer significantly altered exon levels.

697

t-test p-value	*w^{1118} GH* vs			
Exon	*w^{1118} SH*	*$Or47b^{1}$*	*$Or67d^{GAL4}$*	*fru^{LexA}/fru^{4-40}*
P1 (1)	0.5696	0.0316	0.0619	0.0764
Male (2)	0.6843	0.0292	0.0125	0.0013
Female (3)	0.0697	0.3486	0.6932	0.5993
P2 (4)	Expression too low to calculate			
P6 (5)	Expression too low to calculate			
P3 (6)	Expression too low to calculate			
Exon 7 (7)	Expression too low to calculate			
Exon 8 (8)	Expression too low to calculate			
PD (9)	Expression too low to calculate			
P4 (10)	0.8788	0.0387	0.3002	0.1493
P5 (11)	Expression too low to calculate			
C1 (12)	0.5489	0.0117	0.1050	0.0498
C2 (13)	0.6455	0.0826	0.0007	0.0079
C3 (14)	0.3622	0.1247	0.0399	0.0650
C4 (15)	0.8295	0.3811	0.0704	0.1205
D (16)	0.7090	0.2796	0.2787	0.7042
C5 (17)	0.7575	0.7338	0.2378	0.3174
3'UTR (18)	0.7235	0.0086	0.0754	0.1328
FruA (19)	0.5241	0.0498	0.0171	0.0878
FruB (20)	0.8142	0.4809	0.7873	0.2550
FruMC male (21)	0.8519	0.1819	0.1969	0.1943
FruFC female (22)	0.4168	0.1123	0.8214	0.0223

698

699 ## Quantitative reverse transcription PCR (qRT-PCR)

700 The qRT-PCR protocol was modified based on the previous protocol of the Volkan lab (Li et al.,
701 2016). For each genotype, four biological replicates were prepared separately, with each
702 replicate containing 100 antennae from 50 males (7d old). Total antennae RNA was extracted
703 using the RNeasy Mini Kit (QIAGEN, 74104) and treated with DNase I (TURBO DNA-free Kit,
704 Invitrogen, Thermo Fisher Scientific AM1907) to remove genome DNA. cDNA was generated
705 from the reverse transcription of 80-150ng total RNA using the SuperScript IV First-Strand
706 Synthesis Kit (Invitrogen, 18091050) and poly d(T) as transcription primers. qPCR was
707 performed using the FastStart Essential DNA Green Master kit (Roche, 06924204001) on
708 LightCycler® 96 instrument (Roche, 05815916001). The primers are listed in table 1. The
709 expression level was calculated by ΔCt method using the fl(2)d as the standard gene. The
710 calculation was performed in GraphPad Prism software.

711

712 Primers Sets used in qRT-PCR assays:

Primer Names (F: Forward; R: Reverse)	Sequences
fl(2)d set15 F (exon spanning)	AGAAATCGCAGTCGGAGTT
fl(2)d set15 R	CCTTCTCAAGCGTTTGTATGC
wkd set34 F	AATGTGCTAAAGGCCTACTC
wkd set34 R (exon spanning)	TGCAGGTATACATCGCACA
ppk25 set11 F (exon spanning)	CTGCAGTATTACAGTCCCTACC
ppk25 set11 R	TCCGGATACTGTGCAGATTG
5-HT2A set15 F (exon spanning)	CCGTTCTTGGTCTGGTCAAT
5-HT2A set15 R	CGTCAATGCGTATGTGGTAAC
Jheh3 set10 F (exon spanning)	GACCGAAATTCAGGGCTTG
Jheh3 set10 R	GGTTAGCATGGGTATAAAGTCG
fru SM set7 F	ATGGGCACCTGCACAGC
fru SM set7 R	TGCCCGCACATCCGTTT
fru SF set1 F	TGAGAATTCGAGGACGTGTG
fru SF set1 R	GTTCGGGTTGAGTGTTGATTG
fru C1 set1 F	AGGAGCGATGGACCAGCAATTC
fru C1 set1 R	TTGACTGTTTCGCCCTCGCA
fru C2 set2 F	ACAGAACCAGCATCCACATCC
fru C2 set2 R	CTCGGCCGTCTTGAGAAACAT
fru C3 set2 F	GCAGCTGGATTATAGCAACAAGGA
fru C3 set2 R	CTCCCTATTGCTGCTGCTGTT
fru C4 set1 F	TGACCACAAGCGTTCATCT

fru C4 set1 R	CCATCAGCTCCTGCTTGA
fru exonD set7 F	CGTCAACCACCACAACAA
fru exonD set7 R	CTTGCCCACATTTATGGTGA
fru C5 set2_2 F	ACGCGGAGGATATGTCAA
fru C5 set2_2 R	GTCCAGCTGCAGTTGTTT
fru C5RA set2_1 F	CACACACACACACTCAAATAC
fru C5RA set2_1 R	GTTCAACGGATTCTTCACATC
fru exonA set6 F	TGGCACCATGCCAATATC
fru exonA set6 R	TCCGCATGCTTGATCTTAC
fru exonB set2 F	CACATCCGCAACCACTAC
fru exonB set2 R	GTACATGGGATGCTTGAACT
fru exonC set4 F	CGCTTGGTTATGGCAATC
fru exonC set4 R	GGTACGACATGGTGTGAT
fru exonCF set1 F	ACCAAGCAGTCAGAAACC
fru exonCF set1 R	GCCGATTACAAGTGGATGTA

Acknowledgement

We are grateful to Liqun Luo and Hongjie Li for for sharing the single cell RNA-seq data from developing ORNs prior to publication. We would like to thank Yetong Huang, George Thomas Barlow, and Paulina Guerra-Schleske for their contributions to sample collection and RNA extraction of samples, and the Volkan lab for help with the manuscript. We thank the Bloomington Stock Center and UNC High Throughput Sequencing Facility for their services.

Funding statement

This study was supported by National Institute of Health grant number R01NS109401 and National Science Foundation award number 2006471 to PCV. Funders had no decisions in the design of the study, collection of the data or analysis, where the publication is submitted or any hand in writing the manuscript. No conflicts of interest are found.

Data availability

All relevant data are within the paper and its Supporting information files. Raw Data will be uploaded to the GEO under embargo pending the submission and acceptance of the data submitted here for publication.

References

Adam J, T. P. 2011. The Worlds of Splicing and Chromatin CollideRNA Processing. InTech. doi:10.5772/19985

Anders S, Reyes A, Huber W. 2012. Detecting differential usage of exons from RNA-seq data. *Genome Res* **22**. doi:10.1101/gr.133744.111

Becnel J, Johnson O, Luo J, Nässel DR, Nichols CD. 2011. The serotonin 5-HT7dro receptor is expressed in the brain of drosophila, and is essential for normal courtship and mating. *PLoS One*. doi:10.1371/journal.pone.0020800

Billeter JC, Villella A, Allendorfer JB, Dornan AJ, Richardson M, Gailey DA, Goodwin SF. 2006. Isoform-specific control of male neuronal differentiation and behavior in Drosophila by the fruitless gene. *Curr Biol* **16**:1063–1076. doi:S0960-9822(06)01500-4 [pii]10.1016/j.cub.2006.04.039

Brovkina M V., Duffié R, Burtis AEC, Clowney EJ. 2021. Fruitless decommissions regulatory elements to implement cell-type-specific neuronal masculinization. *PLoS Genet* **17**. doi:10.1371/JOURNAL.PGEN.1009338

Carrillo RA, Ozkan E, Menon KP, Nagarkar-Jaiswal S, Lee PT, Jeon M, Birnbaum ME, Bellen HJ, Garcia KC, Zinn K. 2015. Control of Synaptic Connectivity by a Network of Drosophila IgSF Cell Surface Proteins. *Cell* **163**:1770–1782. doi:10.1016/j.cell.2015.11.022

Chou YH, Spletter ML, Yaksi E, Leong JCS, Wilson RI, Luo L. 2010. Diversity and wiring variability of olfactory local interneurons in the Drosophila antennal lobe. *Nat Neurosci* **13**. doi:10.1038/nn.2489

Clowney EJ, Iguchi S, Bussell JJ, Scheer E, Ruta V. 2015. Multimodal Chemosensory Circuits Controlling Male Courtship in Drosophila. *Neuron*. doi:10.1016/j.neuron.2015.07.025

760 Curley JP, Jensen CL, Mashoodh R, Champagne FA. 2011. Social influences on neurobiology
761 and behavior: Epigenetic effects during development. *Psychoneuroendocrinology*.
762 doi:10.1016/j.psyneuen.2010.06.005

763 Cushing BS, Kramer KM. 2005. Mechanisms underlying epigenetic effects of early social
764 experience: The role of neuropeptides and steroids. *Neurosci Biobehav Rev*.
765 doi:10.1016/j.neubiorev.2005.04.001

766 Dacks AM, Green DS, Root CM, Nighorn AJ, Wang JW. 2009. Serotonin modulates olfactory
767 processing in the antennal lobe of drosophila. *J Neurogenet* **23**:366–377.
768 doi:10.3109/01677060903085722

769 Dalton JE, Fear JM, Knott S, Baker BS, McIntyre LM, Arbeitman MN. 2013. Male-specific
770 Fruitless isoforms have different regulatory roles conferred by distinct zinc finger DNA
771 binding domains. *BMC Genomics*. doi:10.1186/1471-2164-14-659

772 Dankert H, Wang L, Hoopfer ED, Anderson DJ, Perona P. 2009. Automated monitoring and
773 analysis of social behavior in Drosophila. *Nat Methods*. doi:10.1038/nmeth.1310

774 Demir E, Dickson BJ. 2005. fruitless splicing specifies male courtship behavior in Drosophila.
775 *Cell* **121**:785–794. doi:S0092-8674(05)00407-1 [pii]10.1016/j.cell.2005.04.027

776 Dey S, Chamero P, Peluso JJ, Stowers L, Dey S, Chamero P, Pru JK, Chien M, Ibarra-soria X,
777 Spencer KR, Logan DW, Matsunami H, Peluso JJ, Stowers L. 2015. Cyclic Regulation of
778 Sensory Perception by a Female Hormone Alters Behavior. *Cell*.
779 doi:10.1016/j.cell.2015.04.052

780 Dickson BJ. 2008. Wired for sex: the neurobiology of Drosophila mating decisions. *Science (80-*
781 *)* **322**:904–909. doi:322/5903/904 [pii]10.1126/science.1159276

782 Dweck HK, Ebrahim SA, Thoma M, Mohamed AA, Keesey IW, Trona F, Lavista-Llanos S,

783 Svatos A, Sachse S, Knaden M, Hansson BS. 2015. Pheromones mediating copulation
784 and attraction in Drosophila. *Proc Natl Acad Sci U S A* **112**:E2829-35.
785 doi:10.1073/pnas.1504527112

786 Eden E, Lipson D, Yogev S, Yakhini Z. 2007. Discovering motifs in ranked lists of DNA
787 sequences. *PLoS Comput Biol*. doi:10.1371/journal.pcbi.0030039

788 Eden E, Navon R, Steinfeld I, Lipson D, Yakhini Z. 2009. GOrilla: A tool for discovery and
789 visualization of enriched GO terms in ranked gene lists. *BMC Bioinformatics*.
790 doi:10.1186/1471-2105-10-48

791 Ellis LL, Carney GE. 2010. Mating alters gene expression patterns in Drosophila melanogaster
792 male heads. *BMC Genomics*. doi:10.1186/1471-2164-11-558

793 Flavell SW, Greenberg ME. 2008. Signaling mechanisms linking neuronal activity to gene
794 expression and plasticity of the nervous system. *Annu Rev Neurosci*.
795 doi:10.1146/annurev.neuro.31.060407.125631

796 Goodwin SF, Taylor BJ, Villella A, Foss M, Ryner LC, Baker BS, Hall JC. 2000. Aberrant
797 splicing and altered spatial expression patterns in fruitless mutants of Drosophila
798 melanogaster. *Genetics* **154**:725–745.

799 Goulding SE, zur Lage P, Jarman AP. 2000. amos, a proneural gene for Drosophila olfactory
800 sense organs that is regulated by lozenge. *Neuron* **25**:69–78.

801 Hueston CE, Olsen D, Li Q, Okuwa S, Peng B, Wu J, Volkan PC. 2016. Chromatin Modulatory
802 Proteins and Olfactory Receptor Signaling in the Refinement and Maintenance of Fruitless
803 Expression in Olfactory Receptor Neurons. *PLoS Biol* **14**.
804 doi:10.1371/journal.pbio.1002443

805 Ito H, Sato K, Koganezawa M, Ote M, Matsumoto K, Hama C, Yamamoto D. 2012. Fruitless

806 recruits two antagonistic chromatin factors to establish single-neuron sexual dimorphism.
807 *Cell*. doi:10.1016/j.cell.2012.04.025

808 Ito H, Sato K, Yamamoto D. 2013. Sex-switching of the Drosophila brain by two antagonistic
809 chromatin factors. *Fly (Austin)* **7**:87–91. doi:10.4161/fly.24018

810 Johnson O, Becnel J, Nichols CD. 2011. Serotonin receptor activity is necessary for olfactory
811 learning and memory in Drosophila melanogaster. *Neuroscience*.
812 doi:10.1016/j.neuroscience.2011.06.058

813 Johnson O, Becnel J, Nichols CD. 2009. Serotonin 5-HT2 and 5-HT1A-like receptors
814 differentially modulate aggressive behaviors in Drosophila melanogaster. *Neuroscience*
815 **158**:1292–1300. doi:10.1016/j.neuroscience.2008.10.055

816 Khlebodarova TM, Gruntenko NE, Grenback LG, Sukhanova MZ, Mazurov MM, Rauschenbach
817 IY, Tomas BA, Hammock BD. 1996. A comparative analysis of juvenile hormone
818 metabolyzing enzymes in two species of Drosophila during development. *Insect Biochem*
819 *Mol Biol* **26**:829–835. doi:10.1016/S0965-1748(96)00043-4

820 Kurtovic A, Widmer A, Dickson BJ. 2007. A single class of olfactory neurons mediates
821 behavioural responses to a Drosophila sex pheromone. *Nature* **446**:542–546.
822 doi:nature05672 [pii]10.1038/nature05672

823 Lee G, Foss M, Goodwin SF, Carlo T, Taylor BJ, Hall JC. 2000. Spatial, temporal, and sexually
824 dimorphic expression patterns of the fruitless gene in the Drosophila central nervous
825 system. *J Neurobiol* **43**:404–426. doi:10.1002/1097-4695(20000615)43:4<404::AID-
826 NEU8>3.0.CO;2-D [pii]

827 Li H, Li T, Horns F, Li J, Xie Q, Xu C, Wu B, Kebschull JM, McLaughlin CN, Kolluru SS, Jones
828 RC, Vacek D, Xie A, Luginbuhl DJ, Quake SR, Luo L. 2020. Single-Cell Transcriptomes

829 Reveal Diverse Regulatory Strategies for Olfactory Receptor Expression and Axon
830 Targeting. *Curr Biol* **30**:1189-1198.e5. doi:10.1016/j.cub.2020.01.049

831 Li Q, Barish S, Okuwa S, Maciejewski A, Brandt AT, Reinhold D, Jones CD, Volkan PC. 2016. A
832 Functionally Conserved Gene Regulatory Network Module Governing Olfactory Neuron
833 Diversity. *PLoS Genet* **12**:e1005780. doi:10.1371/journal.pgen.1005780

834 Lin HH, Cao DS, Sethi S, Zeng Z, Chin JS, Chakraborty TS, Shepherd AK, Nguyen CA, Yew
835 JY, Su CY, Wang JW. 2016. Hormonal Modulation of Pheromone Detection Enhances
836 Male Courtship Success. *Neuron* **90**:1272–1285. doi:10.1016/j.neuron.2016.05.004

837 Liu W, Liang X, Gong J, Yang Z, Zhang YH, Zhang JX, Rao Y. 2011. Social regulation of
838 aggression by pheromonal activation of Or65a olfactory neurons in Drosophila. *Nat*
839 *Neurosci* **14**. doi:10.1038/nn.2836

840 Liu Z, Li X, Prasifka JR, Jurenka R, Bonning BC. 2008. Overexpression of Drosophila juvenile
841 hormone esterase binding protein results in anti-JH effects and reduced pheromone
842 abundance. *Gen Comp Endocrinol*. doi:10.1016/j.ygcen.2008.01.006

843 McGowan PO, Sasaki A, D'Alessio AC, Dymov S, Labonte B, Szyf M, Turecki G, Meaney MJ.
844 2009. Epigenetic regulation of the glucocorticoid receptor in human brain associates with
845 childhood abuse. *Nat Neurosci* **12**:342–348. doi:10.1038/nn.2270

846 McLaughlin CN, Brbić M, Xie Q, Li T, Horns F, Kolluru SS, Kebschull JM, Vacek D, Xie A, Li J,
847 Jones RC, Leskovec J, Quake SR, Luo L, Li H. 2021. Single-cell transcriptomes of
848 developing and adult olfactory receptor neurons in drosophila. *Elife* **10**.
849 doi:10.7554/eLife.63856

850 Meier N, Kappeli SC, Hediger Niessen M, Billeter JC, Goodwin SF, Bopp D. 2013. Genetic
851 control of courtship behavior in the housefly: evidence for a conserved bifurcation of the

852 sex-determining pathway. *PLoS One* **8**:e62476. doi:10.1371/journal.pone.0062476

853 Mellert DJ, Knapp JM, Manoli DS, Meissner GW, Baker BS. 2010. Midline crossing by gustatory
854 receptor neuron axons is regulated by fruitless, doublesex and the Roundabout receptors.
855 *Development* **137**:323–332. doi:10.1242/dev.045047

856 Mifsud KR, Gutierrez-Mecinas M, Trollope AF, Collins A, Saunderson EA, Reul JM. 2011.
857 Epigenetic mechanisms in stress and adaptation. *Brain Behav Immun* **25**:1305–1315.
858 doi:10.1016/j.bbi.2011.06.005

859 Mohamed AAM, Retzke T, Das Chakraborty S, Fabian B, Hansson BS, Knaden M, Sachse S.
860 2019. Odor mixtures of opposing valence unveil inter-glomerular crosstalk in the
861 Drosophila antennal lobe. *Nat Commun* **10**. doi:10.1038/s41467-019-09069-1

862 Naftelberg S, Schor IE, Ast G, Kornblihtt AR. 2015. Regulation of alternative splicing through
863 coupling with transcription and chromatin structure. *Annu Rev Biochem*.
864 doi:10.1146/annurev-biochem-060614-034242

865 Neville MC, Nojima T, Ashley E, Parker DJ, Walker J, Southall T, Van de Sande B, Marques
866 AC, Fischer B, Brand AH, Russell S, Ritchie MG, Aerts S, Goodwin SF. 2014. Male-
867 specific fruitless isoforms target neurodevelopmental genes to specify a sexually dimorphic
868 nervous system. *Curr Biol* **24**:229–241. doi:10.1016/j.cub.2013.11.035

869 Ng R, Salem SS, Wu ST, Wu M, Lin HH, Shepherd AK, Joiner WJ, Wang JW, Su CY. 2019.
870 Amplification of Drosophila Olfactory Responses by a DEG/ENaC Channel. *Neuron*.
871 doi:10.1016/j.neuron.2019.08.041

872 Nojima T, Neville MC, Goodwin SF. 2014. Fruitless isoforms and target genes specify the
873 sexually dimorphic nervous system underlying Drosophila reproductive behavior. *Fly*
874 *(Austin)* **8**.

875 Olsen SR, Bhandawat V, Wilson RI. 2007. Excitatory Interactions between Olfactory Processing
876 Channels in the Drosophila Antennal Lobe. *Neuron* **54**. doi:10.1016/j.neuron.2007.03.010

877 Pikielny CW. 2012. Sexy DEG/ENaC channels involved in gustatory detection of fruit fly
878 pheromones. *Sci Signal*. doi:10.1126/scisignal.2003555

879 Root CM, Masuyama K, Green DS, Enell LE, Nassel DR, Lee CH, Wang JW. 2008. A
880 presynaptic gain control mechanism fine-tunes olfactory behavior. *Neuron* **59**:311–321.
881 doi:S0896-6273(08)00572-2 [pii]10.1016/j.neuron.2008.07.003

882 Ryner LC, Goodwin SF, Castrillon DH, Anand A, Villella A, Baker BS, Hall JC, Taylor BJ,
883 Wasserman SA. 1996. Control of male sexual behavior and sexual orientation in
884 Drosophila by the fruitless gene. *Cell*. doi:10.1016/S0092-8674(00)81802-4

885 Sato K, Yamamoto D. 2020. The mode of action of Fruitless: Is it an easy matter to switch the
886 sex? *Genes, Brain Behav*. doi:10.1111/gbb.12606

887 Scanlan JL, Gledhill-Smith RS, Battlay P, Robin C. 2020. Genomic and transcriptomic analyses
888 in Drosophila suggest that the ecdysteroid kinase-like (EcKL) gene family encodes the
889 'detoxification-by-phosphorylation' enzymes of insects. *Insect Biochem Mol Biol* **123**.
890 doi:10.1016/j.ibmb.2020.103429

891 Seong KM, Coates BS, Berenbaum MR, Clark JM, Pittendrigh BR. 2018. Comparative CYP-
892 omic analysis between the DDT-susceptible and -resistant Drosophila melanogaster strains
893 91-C and 91-R. *Pest Manag Sci* **74**. doi:10.1002/ps.4936

894 Seong KM, Coates BS, Pittendrigh BR. 2019. Cytochrome P450s Cyp4p1 and Cyp4p2
895 associated with the DDT tolerance in the Drosophila melanogaster strain 91-R. *Pestic*
896 *Biochem Physiol* **159**. doi:10.1016/j.pestbp.2019.06.008

897 Sethi S, Lin HH, Shepherd AK, Volkan PC, Su CY, Wang JW. 2019. Social Context Enhances

898 Hormonal Modulation of Pheromone Detection in Drosophila. *Curr Biol* **29**:3887–3898.
899 doi:10.1016/j.cub.2019.09.045

900 Sizemore TR, Dacks AM. 2016. Serotonergic Modulation Differentially Targets Distinct Network
901 Elements within the Antennal Lobe of Drosophila melanogaster. *Sci Rep* **6**.
902 doi:10.1038/srep37119

903 Sudhakaran IP, Holohan EE, Osman S, Rodrigues V, Vijay Raghavan K, Ramaswami M. 2012.
904 Plasticity of recurrent inhibition in the Drosophila antennal lobe. *J Neurosci* **32**:7225–7231.
905 doi:10.1523/JNEUROSCI.1099-12.2012

906 Suzuki Y, Schenk JE, Tan H, Gaudry Q. 2020. A Population of Interneurons Signals Changes in
907 the Basal Concentration of Serotonin and Mediates Gain Control in the Drosophila
908 Antennal Lobe. *Curr Biol*. doi:10.1016/j.cub.2020.01.018

909 Usui-Aoki K, Ito H, Ui-Tei K, Takahashi K, Lukacsovich T, Awano W, Nakata H, Piao ZF,
910 Nilsson EE, Tomida J, Yamamoto D. 2000. Formation of the male-specific muscle in
911 female Drosophila by ectopic fruitless expression. *Nat Cell Biol* **2**:500–506.
912 doi:10.1038/35019537

913 van der Goes van Naters W, Carlson JR. 2007. Receptors and neurons for fly odors in
914 Drosophila. *Curr Biol* **17**:606–612. doi:S0960-9822(07)01020-2
915 [pii]10.1016/j.cub.2007.02.043

916 Vernes SC. 2014. Genome wide identification of Fruitless targets suggests a role in
917 upregulating genes important for neural circuit formation. *Sci Rep*. doi:10.1038/srep04412

918 Von Philipsborn AC, Jörchel S, Tirian L, Demir E, Morita T, Stern DL, Dickson BJ. 2014. Cellular
919 and behavioral functions of fruitless isoforms in Drosophila courtship. *Curr Biol*.
920 doi:10.1016/j.cub.2013.12.015

921 Wang JW, Wong AM, Flores J, Vosshall LB, Axel R. 2003. Two-photon calcium imaging reveals
922 an odor-evoked map of activity in the fly brain. *Cell* **112**. doi:10.1016/S0092-
923 8674(03)00004-7

924 Wang L, Dankert H, Perona P, Anderson DJ. 2008. A common genetic target for environmental
925 and heritable influences on aggressiveness in Drosophila. *Proc Natl Acad Sci U S A*.
926 doi:10.1073/pnas.0801327105

927 Wang L, Han X, Mehren J, Hiroi M, Billeter JC, Miyamoto T, Amrein H, Levine JD, Anderson DJ.
928 2011. Hierarchical chemosensory regulation of male-male social interactions in Drosophila.
929 *Nat Neurosci* **14**:757–762. doi:nn.2800 [pii]10.1038/nn.2800

930 Weaver IC, Cervoni N, Champagne FA, D'Alessio AC, Sharma S, Seckl JR, Dymov S, Szyf M,
931 Meaney MJ. 2004. Epigenetic programming by maternal behavior. *Nat Neurosci* **7**:847–
932 854. doi:10.1038/nn1276

933 West AE, Greenberg ME. 2011. Neuronal activity-regulated gene transcription in synapse
934 development and cognitive function. *Cold Spring Harb Perspect Biol* **3**.
935 doi:cshperspect.a005744 [pii]10.1101/cshperspect.a005744

936 Wilson RI. 2013. Early olfactory processing in drosophila: Mechanisms and principles. *Annu*
937 *Rev Neurosci*. doi:10.1146/annurev-neuro-062111-150533

938 Wong AM, Wang JW, Axel R. 2002. Spatial representation of the glomerular map in the
939 Drosophila protocerebrum. *Cell* **109**. doi:10.1016/S0092-8674(02)00707-9

940 Yamamoto D. 2007. The neural and genetic substrates of sexual behavior in Drosophila. *Adv*
941 *Genet* **59**:39–66. doi:10.1016/S0065-2660(07)59002-4

942 Yamamoto D, Koganezawa M. 2013. Genes and circuits of courtship behaviour in Drosophila
943 males. *Nat Rev Neurosci* **14**:681–692. doi:10.1038/nrn3567

944 Yamamoto D, Kohatsu S. 2017. What does the fruitless gene tell us about nature vs. nurture in
945 the sex life of Drosophila? *Fly (Austin)*. doi:10.1080/19336934.2016.1263778

946 Yamamoto D, Kohatsu S, Koganezawa M. 2013. Insect pheromone behavior: fruit fly. *Methods*
947 *Mol Biol* **1068**:261–272. doi:10.1007/978-1-62703-619-1_19

948 Yan H, Jafari S, Pask G, Zhou X, Reinberg D, Desplan C. 2020. Evolution, developmental
949 expression and function of odorant receptors in insects. *J Exp Biol*. doi:10.1242/jeb.208215

950 Zhang X, Coates K, Dacks A, Günay C, Lauritzen JS, Li F, Calle-Schuler SA, Bock D, Gaudry
951 Q. 2019. Local synaptic inputs support opposing, network-specific odor representations in
952 a widely projecting modulatory neuron. *Elife* **8**. doi:10.7554/eLife.46839

953 Zhang Y, Ng R, Neville MC, Goodwin SF, Su CY. 2020. Distinct Roles and Synergistic Function
954 of FruM Isoforms in Drosophila Olfactory Receptor Neurons. *Cell Rep* **33**.
955 doi:10.1016/j.celrep.2020.108516

956 Zhang Y, Su C-Y. 2020. Distinct Roles and Synergistic Function of Fru ^{M} Isoforms in *Drosophila*
957 Olfactory Receptor Neurons. *SSRN Electron J*. doi:10.2139/ssrn.3624384

958 Zhao S, Deanhardt B, Barlow GT, Schleske PG, Rossi AM, Volkan PC. 2020. Chromatin-based
959 reprogramming of a courtship regulator by concurrent pheromone perception and hormone
960 signaling. *Sci Adv* **6**:eaba6913. doi:10.1126/sciadv.aba6913

961 zur Lage PI, Prentice DR, Holohan EE, Jarman AP. 2003. The Drosophila proneural gene amos
962 promotes olfactory sensillum formation and suppresses bristle formation. *Development*
963 **130**:4683–4693. doi:10.1242/dev.00680130/19/4683 [pii]

964